NASA TECHNICAL NOTE

NASA TN D-2937

c. 1

NASA TN D-2937

WIND VELOCITY PROFILES MEASURED BY THE SMOKE-TRAIL METHOD AT WALLOPS ISLAND, VIRGINIA, 1959 TO 1962

by Robert W. Miller, Robert M. Henry, and Mickey G. Rowe

Langley Research Center
Langley Station, Hampton, Va.

NATIONAL AERONAUTICS AND SPACE ADMINISTRATION • WASHINGTON, D. C. • AUGUST 1965

NASA TN D-2937

WIND VELOCITY PROFILES MEASURED BY THE SMOKE-TRAIL METHOD AT WALLOPS ISLAND, VIRGINIA, 1959 TO 1962

By Robert W. Miller, Robert M. Henry,
and Mickey G. Rowe

Langley Research Center
Langley Station, Hampton, Va.

NATIONAL AERONAUTICS AND SPACE ADMINISTRATION

For sale by the Clearinghouse for Federal Scientific and Technical Information
Springfield, Virginia 22151 – Price $3.00

WIND VELOCITY PROFILES MEASURED BY THE SMOKE-TRAIL METHOD AT WALLOPS ISLAND, VIRGINIA, 1959 TO 1962

By Robert W. Miller, Robert M. Henry,
and Mickey G. Rowe
Langley Research Center

SUMMARY

Twenty-three detailed wind profiles measured by the smoke-trail technique at Wallops Island, Virginia, during the years 1959 to 1962 are presented as plots of west-to-east and south-to-north velocity components at height intervals of 25 meters. The altitude ranges of individual profiles vary, but the overall range is roughly 2 to 20 kilometers. The measurements were made under a wide variety of weather conditions, including one case with an exceptionally high maximum wind. Modifications of the measurement technique and accuracy of the profiles are discussed.

INTRODUCTION

The smoke-trail wind-measurement technique described in reference 1 was developed to supply accurate measurements of the small-scale variations of wind velocity with altitude. Knowledge of these small-scale variations is needed for dynamic-response studies of vertically launched missile and space systems and for other purposes. The small-scale variations cannot be obtained from present-day conventional balloon-sounding methods because of tracking errors, unstable or self-induced motions of the balloons, and the horizontal drift of the balloons during ascent.

In 1959 a feasibility study of the measurement of wind velocity profiles by the use of smoke trails was undertaken at Wallops Station, Wallops Island, Virginia. This study was followed by a system development program, which was concluded in 1962 and which resulted in the present smoke-trail wind-measurement technique. In August 1963, a series of 70 firings was begun for the purpose of obtaining a limited climatological sample of detailed wind profiles at the Wallops Island range. In addition to this program, a series of 108 firings was begun at the Eastern Test Range in May 1962 in order to obtain a climatological sample at that location.

The 23 smoke-trail wind velocity profiles in the present report were obtained from the feasibility study and the system development program, together with a few firings undertaken in support of other missions. Several of the wind profiles have been reported in references 1 to 11 but a complete set of profiles has not previously been available for general use. The purpose of this publication is to make available the basic data obtained from smoke-trail measurements at Wallops Station from 1959 to 1962.

MEASUREMENT TECHNIQUE

The basic technique for obtaining detailed wind profiles from smoke trails consists of photographing a visible trail formed by releasing a suitable chemical from a rocket during the coasting portion of its flight and determining the motion of the trail from photogrammetric measurements. The fundamental procedures are described fully in reference 1 and more briefly in references 2 to 4. The present report discusses only changes in or additions to the procedures.

The Smoke Rocket

The data in the present report were derived from smoke trails produced by a variety of rocket vehicles, including operational and experimental systems. Several experimental systems, including smaller rockets and a separating payload, were tested during the course of development of the smoke-trail method. Smaller rockets such as ARCAS are capable of producing a trail that is sufficiently dense but too narrow to be visible in the required photographs. Use of a separating payload with the Nike rocket was successful but involves additional cost and range support requirements. The rocket in current use is essentially a standard Nike with a nose cone modified as described in reference 12.

Smoke-Producing Chemicals

The smoke-producing chemical presently being used is titanium tetrachloride (FM). Although slightly less efficient at low altitudes than the solution of sulfur trioxide in chlorosulfonic acid (FS) originally used, it is much more effective at the higher altitudes. A slight disadvantage of the titanium tetrachloride is delay in the formation of the visible trail. It required 2 to 3 minutes to achieve full brightness in the vicinity of 2 kilometers. A superconcentrated solution of phosphorus in carbon disulphide (85 percent phosphorus by weight) was also flight-tested and produced excellent results. It formed a bright persistent trail with no detectable time delay. However, phosphorus is not used routinely because of handling difficulties. Pyrotechnic smoke-producing mixtures were ground-tested but were found to be unsuited to the present application. Details of the smoke-agent tests may be found in reference 13.

Data Preparation

Because of the interest in small-scale features of the profile, a great deal of attention must be given to the avoidance of random errors or stray points which might ordinarily be of little concern, but which in the present application might be erroneously interpreted as real small-scale features of the atmosphere. Although they are extremely time consuming, the painstaking checking procedures outlined below have been found to be essential to the production of data which are satisfactory for structural-dynamic studies. A number of checking procedures have been incorporated in the computer program, but many checks still depend upon human judgment. The steps in preparing the data for machine processing follow.

Time synchronization check.- Although the timers used to synchronize the operation of the camera shutters provide timing accurate to a fraction of a second, the recorded frame number may be in error by a whole number, with a resulting error which is a multiple of the 6-second timing interval used at the Wallops Island range. Time synchronization is checked by comparing the position of the rocket image on the various photographs and finally by checking consistency of apparent motion of the trail on successive photographs.

Selection of photographs.- The camera having the most readable photographs from the pair of cameras at each site is selected and the 1-minute interval having the most readable trail is chosen from the various possible combinations. Three pairs of simultaneous pictures at successive 30-second intervals are then read.

Film reading and editing.- In each picture, the coordinates of the fiducial marks, calibrated-focal-length marks, and surveyed camera orientation reference marks are read five times each. These readings are averaged to reduce reading error. The trail image in each picture selected is read twice. Because these smoke-trail point readings are not made at fixed intervals, they cannot be averaged, or compared point by point. In order to compare the two corresponding readings, the trail-image coordinates are machine plotted, and compared by superimposing one plot on another, the plotted fiducial marks being alined. Any discrepancy between the two readings is checked and corrected. In addition to checking one reading against another reading of the same photograph, the consistency of movement of the trail coordinates for the successive 30-second intervals is checked, and the plotted trail coordinates are compared visually with the photographs. After all these checks have been made, one corrected reading of the trail coordinates from each of the six photographs is selected for further processing.

Data Reduction

The data reduction procedure is basically the same as that given in reference 1. Additional subroutines have been incorporated to perform an additional coordinate rotation necessitated by a change in surveyed reference arrangements and to minimize the effects of any erroneous points which may still be present in spite of previous checking procedures.

Coordinate rotation.- In the camera orientation and coordinate rotation procedure of reference 1, the cameras and surveyed reference marks were all assumed to lie in a common horizontal plane. When new camera sites were established, such an arrangement was not convenient; therefore, another coordinate rotation step was added to rotate from the local vertical at each camera station to the local vertical midway between cameras. Thus, the horizontal plane of the final coordinate system is perpendicular to the vertical at the midpoint of the base line and passes through the camera locations.

Machine editing.- Early in the smoke-trail program, it was discovered that a single "wild point" could sometimes cause the program to bypass a large number of correct points or even produce an incorrect matching of points in the two pictures. This error could result in computation of the coordinates of one of the extraneous ray intersections which is a mathematically correct solution, but is not the physically correct solution corresponding to the actual smoke-trail position. Since this situation could occur as a result of even small errors, such as the operator inadvertently backtracking along the trail (an error which could not be detected by the visual reading check), a series of machine operations was devised to prevent such occurrences. The effect of these operations, which are described in detail in appendix A, is to reject any point where the elevation angle in the rotated coordinate system appears to be increasing in one picture but decreasing in the other, and also to reject any point where the computed height of the trail would decrease along the trail, as followed in the order of its formation. Although it is clear that all the points so rejected would have resulted in incorrect velocity computation, it is not possible to determine what the correct value would have been. Therefore, a linear interpolation is performed between the last correct point and the next correct point. With the very large number of points read, this method does not usually result in appreciable error, but the possibility of such errors cannot be completely eliminated.

DISCUSSION OF DATA

The Langley trail identification number, date, time, altitude range, and maximum west-to-east wind component for each profile are listed in table I. The altitude ranges of the individual profiles vary, but the overall range is roughly 2 to 20 kilometers. A number of the profiles cover a limited altitude range, but have been included to make the report complete. The wind profile data are presented in figures 1 to 23 in the form of plots of west-to-east and south-to-north components of velocity as a function of altitude. West-to-east and south-to-north velocities are positive. Wind components are evaluated at altitude intervals of 25 meters, except for the first three profiles for which slightly different intervals were used.

On request from the NASA Langley Research Center, the same data, plus wind speed and direction and wind-shear values, are also available on punched cards or in tabular form.* The format of the data and the units used are illustrated by the sample tabulation in table II. In tabular form each profile is identified by a trail number, date and time of launch, altitude increment used in computation, time increments over which the data were taken, and camera and picture identification. The various measures of the wind shear, or rate of change of wind velocity with height, are evaluated over a height interval of 25 meters

*Requests should be directed to the Langley Research Center and the paper cited by author, title, and code number, together with specific profiles desired.

and apply to the 25-meter height interval immediately below the reported height. Wind-shear values have been included in the tabulations because of numerous requests. However, the user should be aware of the large errors involved in computation of shears over an interval as small as 25 meters. For example, a root-mean-square (rms) velocity error of 1.0 m/sec would result in an rms shear error of 0.056 sec^{-1}. (Actual shear values as large as 0.056 sec^{-1} are seldom encountered.) Of course, the magnitude of the error decreases in proportion to the altitude interval used; thus, some users may find it desirable to average several of the reported values or to compute directly the shears over larger altitude intervals.

Radiosonde runs were made within 6 hours of each of the smoke-trail firings, but since meteorological studies generally also require data from other stations, the results have not been included in this report. Radiosonde or other data are available from the National Weather Records Center, U.S. Weather Bureau, Federal Building, Asheville, North Carolina 28801.

The primary purpose of the smoke-trail wind measurement program is to provide data for use in the study of the structural dynamics of ascending rocket vehicle systems. However, because data of this type are of interest for a number of applications and because wind data of comparable accuracy and detail are limited, all the usable profiles which were measured at Wallops Island during the period covered by this report are included even though some may cover too small an altitude range to be of value for vehicle simulation studies.

Significant Features

Because the response of different rocket vehicles to wind excitation varies greatly, no attempt is made to rank the profiles in order of severity. However, certain features of some of the profiles, which are of particular interest from the viewpoint of structural dynamics in that they might produce high loads on some vehicle configurations and which are also of general interest, may be pointed out.

In the profile of trail 004 (fig. 3), unusually large values of wind shear are found in the region of 5 to 6 kilometers. These high wind-shear values appear to coincide with the position of an intense cold front whose surface position lies southeast of the launch site.

In trail 008 (fig. 7), the pair of spikes in both the west-to-east and south-to-north profiles at 11.5 and 12.5 kilometers appear to be of particular interest in that they might produce very high loads on some vehicles.

An outstanding feature in trail 009 (fig. 8) is the large maximum wind at 11 kilometers. This peak value is larger than 99 percent of the peak values at Wallops Island during the month of highest winds and higher than 99.9 percent of the peak values for the entire year, based on the wind statistics in reference 14. Also of interest is the series of approximately step increases in velocity leading up to the maximum.

In trail 020 (fig. 16), two sharp spikes appear in the south-to-north component at 7 and 11 kilometers, one of positive sign and the other of negative sign. In trail 021 (fig. 17), a series of very sharp spikes appears in the higher altitudes. In trail 027 (fig. 23), an irregular pattern exists over most of the trail, but between 12 and 14 kilometers a remarkably uniform shear is found. It should not, of course, be inferred that these features are necessarily more important, or produce greater vehicle loads for all types of vehicles than other features of less striking appearance.

Accuracy

The degree of detail and accuracy of the smoke-trail data is substantially better than that of data obtained with other present-day conventional measuring systems. The present discussion is directed toward the accuracy of the particular profiles included in this report. For considerations of the accuracy of the measurement system, the reader is referred to the extensive discussion in reference 1 and the briefer discussions in references 2 and 3.

Reference 1 shows that the error in wind velocity is directly proportional to the total film-coordinate error and inversely proportional to the time interval and to the camera focal length, that it increases with altitude, and that it is a rather complicated function of the position and slope of the trail and of camera orientation angles. For the actual Wallops Island camera network, a typical trail position, and the rather ideal simplifying condition of a vertical trail, the rms velocity error is

$$\sigma_V = 345\ 600\sigma_r/\Delta t \tag{1}$$

in nondimensional form, where σ_V is the rms vector error of wind velocity, σ_r the rms film-coordinate error, and Δt the time interval. Equation (1) can also be written

$$\sigma_V = 0.3456\sigma_r/\Delta t \tag{2}$$

where σ_V is in m/sec, σ_r in microns, and Δt in seconds, or (in the units of ref. 1)

$$\sigma_V = 28\ 800\sigma_r/\Delta t \tag{3}$$

where σ_V is in ft/sec, σ_r in inches, and Δt in seconds. Reference 1 indicated that the rms errors determined by comparison of calculations from independent pairs of photographs for sample trails were in reasonable agreement with the theoretical values.

In reference 1 the film-reading accuracy obtained with actual trails under typical conditions, for the 1-minute time interval, yielded theoretical rms velocity errors as low as 0.1 m/sec. Of course, in many cases the film-reading accuracy is expected to decrease because of unfavorable meteorological or operational conditions, and position and velocity errors are expected to increase as a result of smoke trails which are not completely vertical.

For several of the cases where larger errors were expected, either because of the conditions of the rocket launching or because of the appearance of the resulting wind profile, calculations were made by using pairs of pictures taken either from different cameras or at different times or both. The rms velocity errors, computed from the independent pairs of photographs, are shown in table III. The accuracy of most of the profiles was on the order of 0.5 to 1 m/sec root mean square.

In interpreting the rms values, it should be noted that winds at the same computed altitude were compared and that the computed altitudes may be in error by about 100 meters at the higher altitudes. Thus, for regions of high shear, a large rms error may be reported simply as a result of a small vertical displacement of one of the wind profiles; however, this type of error would not be of importance for most uses of the data. Errors of this type are not included in the theoretical error values of equation (1) in the present report nor in the complete error equations in reference 1.

The first entry in table III, trail 008, represents a case which was far from ideal in many respects. This profile was derived from the exhaust trail of a Scout vehicle rather than from the trail of the coasting Nike ordinarily used. The trail was rather wide and irregular, and the rocket trajectory was such as to produce considerable deviation from the vertical at the higher altitudes reported. In addition, one of the camera stations was in the process of relocation and target boards had not been installed. Nevertheless, errors are small at the lower altitudes and reach 2 m/sec only at altitudes above 13 kilometers.

Trail 009 illustrates the effect of extremely high winds. In the altitude range of the present study, the maximum vector wind was nearly 100 m/sec, higher than 99 percent of the winds in the month of highest winds and higher than 99.9 percent of the winds during the entire year. The effect of the rapid departure of the trail from vertical because of the strong shear can be seen from the fact that the rms errors of the 60-second profiles, although not excessively large, are about the same size as those of the 30-second profile, whereas in the usual case they are only half as large.

Trail 018 showed one sharp spike in the south-to-north component at about 5 kilometers, but it appeared questionable and was removed; otherwise this trail was a normal one, obtained under more or less average conditions, and is expected to be representative of the normal errors. These error values are only slightly larger than those derived by the simplified theory of equation (1).

In trails 021 and 027, very complicated wind patterns exist and lead to numerous sharp spikes on the component profiles. These two trails represent the largest errors (1 to 1.5 m/sec root mean square) which would be expected under conditions where satisfactory smoke-trail photography is possible.

In addition to these rms error estimates, rms differences between wind velocities derived from simultaneous smoke trails were computed. Trails 023, 024, and 025 were obtained from three nearly simultaneous launchings of smoke-trail rockets from different launch pads (ref. 13), and differences between the various pairs of trails are shown in table IV. The distances between the trails varied from 0.25 to 2 kilometers. If the variation of wind velocity between trails is neglected and all the difference assigned to measurement error, the error assignable to each measurement would be $1/\sqrt{2}$ (or about 0.7) times the value in table IV. These errors are no larger than those for a single trail.

Representativeness

In addition to giving an indication of measurement accuracy, the small rms differences in table IV between the separate pairs of trails indicate that these smoke-trail measurements can be considered representative of the atmosphere at least over distances of several kilometers, or time intervals of several minutes. Additional measured values and a more extensive discussion of the representativeness of winds as measured by the smoke-trail technique may be found in reference 10.

CONCLUDING REMARKS

Twenty-three detailed wind profiles measured by the smoke-trail technique at Wallops Island during the years 1959 to 1962 were presented. The profiles included west-to-east and south-to-north components determined at 25-meter altitude increments. The altitude ranges of the individual profiles vary, but the overall range is roughly 2 to 20 kilometers. The measurements were made under a wide variety of weather conditions, including exceptionally high maximum winds. Modifications of the measurement technique and accuracy of the profiles are discussed. The accuracy of most of the profiles was on the order of 0.5 to 1 m/sec root mean square. Under unfavorable conditions, rms errors as high as 2 m/sec were found at altitudes above 13 kilometers. This degree of detail and accuracy is substantially better than that of data obtained with other present-day conventional measuring systems and is particularly suited to studies of the structural dynamics of vertically launched vehicle systems.

Langley Research Center,
National Aeronautics and Space Administration,
Langley Station, Hampton, Va., April 19, 1965.

APPENDIX A

MACHINE DATA PROCESSING

Figure 24 is a simplified flow diagram of the data reduction procedures used in reducing the smoke-trail wind-shear and velocity data.

The data-processing personnel enter the sequence of events leading to final answers for the smoke-trail data at step A. This step is a preliminary editing procedure designed to eliminate incorrectly punched cards and discrepancies which would halt the electronic data processing system because of programer checks. The data-processing operator insures that the proper constants are available, arranges the punched cards in the proper order, performs hand editing as indicated on log sheets provided with the punched cards, and uses a collator to check the sequence of the cards and check the cards for double punches or blank columns.

An IBM 1401 electronic data processing system is then used in step B to list the edited punched cards, prepare a data tape for processing by the IBM 7070 electronic data processing system, and prepare a tape for a magnetic-tape plotter. As a quality control measure, the results on the tape are plotted and these plots and a listing of the raw data are returned to the project engineer for checking and editing. As a routine check, each picture of data is read twice on the comparator. Using the plots and the listing, the engineer checks the duplicate readings for similarity and checks successive pictures for continuity with increasing time. At this point the engineer can accept all readings for processing, select certain readings for processing, or direct that all or certain frames be reread for the smoke trail. Steps A and B can then be repeated as necessary.

At step C the data are actually reduced to final answers. Because of the magnetic-tape sort techniques utilized and system core storage limitations, there are six different programs involved in step C. However, the programs may be sequentially loaded with a minimum of operator intervention, each phase being executed as soon as the previous phase is completed. Naturally, if only certain phases are desired, they may be executed individually. The minor operational difficulties resulting from the phasing of the programs are offset by the ease with which intermediate answers can be printed and/or plotted as a quality control measure or as a check on the calculations. Of course, feasible programed checks are included in the system programs to insure that the electronic data processing system is using the correct constants, that the data have been properly edited, and that the frame and camera numbers are being used in the correct sequence. Both the input to and the output of step C are saved for storage to provide a rerun capability in the event of constant changes and to keep the answers available for further use without reprocessing.

Step D serves as an output function. Two special output tapes are prepared — a print tape for the IBM 1401 electronic data processing system and a plot tape for the magnetic-tape plotter. These tapes are printed and plotted and the results are returned to the project engineer.

REFERENCES

1. Henry, Robert M.; Brandon, George W.; Tolefson, Harold B.; and Lanford, Wade E.: The Smoke-Trail Method for Obtaining Detailed Measurements of the Vertical Wind Profile for Application to Missile-Dynamic-Response Problems. NASA TN D-976, 1961.

2. Tolefson, Harold B.; and Henry, Robert M.: A Method of Obtaining Detailed Wind Shear Measurements for Application to Dynamic Response Problems of Missile Systems. J. Geophys. Res., vol. 66, no. 9, Sept. 1961, pp. 2849-2862.

3. Henry, Robert M.; and Brandon, George W., Jr.: The Use of Smoke Trails as Wind Sensors. 1961 Proceedings ISA 16th Annual Instrument-Automation Conference and Exhibit, vol. 16-pt. 2-b, 1961, pp. 174-LA-61-1 - 174-LA-61-16.

4. Tolefson, Harold B.: Smoke-Trail Measurements of the Vertical Wind Profile and Some Applications. Air Force Surv. in Geophys. No. 140 (AFCRL-62-273 (I)), Air Force Cambridge Res. Center, Mar. 1962.

5. Morgan, Homer G.; and Baron, Sheldon: Wind Loads on a Vertically Rising Vehicle Including Effects of Time-Varying Parameters. Structural Dynamics of High Speed Flight, ACR-62, vol. 1, Office of Naval Res., Apr. 1961, pp. 413-446.

6. Baron, Sheldon: Analysis of a Vertically Rising Vehicle. M.A. Thesis, The College of William and Mary, 1961.

7. Morgan, Homer G.; and Collins, Dennis F., Jr.: Some Applications of Detailed Wind Profile Data to Launch Vehicle Response Problems. AIAA Jour., vol. 1, no. 2, Feb. 1963, pp. 368-373.

8. Scoggins, James R.: High Resolution Wind Measurement: A Launch Design Problem. Astronaut. Aerospace Eng., vol. 1, no. 3, Apr. 1963, pp. 106-107.

9. Lester, Harold C.; and Morgan, Homer G.: Determination of Launch-Vehicle Response to Detailed Wind Profiles. Preprint No. 64-82, Am. Inst. Aeron. Astronaut., Jan. 1964.

10. Lester, Harold C.; and Tolefson, Harold B.: A Study of Launch-Vehicle Responses to Detailed Characteristics of the Wind Profile. J. Appl. Meteorol., vol. 3, no. 5, Oct. 1964, pp. 491-498.

11. Murrow, Harold N.; and Henry, Robert M.: Self-Induced Balloon Motions. J. Appl. Meteorol., vol. 4, no. 1, Feb. 1965, pp. 131-138.

12. Lanford, Wade E.; Perry, Tom W., Jr.; Baber, Hal T., Jr.; and Booth, Franklin W.: Development of a Smoke-Trail Vehicle for Application to Wind-Shear Measurements up to 80,000 Feet. NASA TN D-2009, 1963.

13. Lanford, Wade E.; Janos, Joseph, J.; and Baber, Hal T., Jr.: Comparison and Evaluation of Several Chemicals as Agents for Rocket-Vehicle Production of Smoke Trails for Wind-Shear Measurements. NASA TN D-2277, 1964.

14. Weaver, William L.; Swanson, Andrew G.; and Spurling, John F.: Statistical Wind Distribution Data for Use at NASA Wallops Station. NASA TN D-1249, 1962.

TABLE I

WALLOPS ISLAND WIND PROFILES FOR 1959 to 1962 LAUNCHINGS

Figure	Trail identification	Date	Time EST	Altitude range, m	Maximum west-to-east component of velocity, m/sec	Remarks
1	002	9/21/59	1500	2 408 to 11 582	8	
2	003	11/04/59	1040	1 554 to 10 485	67*	Little Joe exhaust trail
3	004	12/04/59	1120	1 803 to 12 177	-12*	Little Joe exhaust trail
4	005	9/08/60	1330	4 025 to 8 825	-8	
5	006	9/23/60	1110	3 425 to 13 400	16	
6	007	2/15/61	1300	2 700 to 9 900	51*	
7	008	2/16/61	0807	1 750 to 18 000	60	Scout exhaust trail
8	009	4/06/61	1435	3 250 to 12 500	93	
9	010	4/14/61	1030	4 600 to 10 175	37*	
10	012	4/14/61	1435	3 175 to 12 400	39	
11	014	7/14/61	1100	11 175 to 13 900	18*	
12	015	7/14/61	1620	4 750 to 14 000	24	
13	016	7/14/61	1620	11 175 to 13 950	24	
14	018	10/24/61	1110	2 600 to 12 250	23*	
15	019	11/22/61	1030	3 175 to 11 775	33	
16	020	1/16/62	1610	3 075 to 15 750	72	
17	021	2/06/62	1400	2 600 to 16 750	65	
18	022	4/04/62	1550	3 050 to 11 425	40*	
19	023	5/04/62	1530	4 000 to 8 875	31*	
20	024	5/04/62	1530	2 800 to 12 275	43	
21	025	5/04/62	1530	2 200 to 18 225	42	
22	026	5/05/62	1340	2 950 to 14 825	19	
23	027	5/25/62	1240	5 000 to 15 000	35	

*Maximum west-to-east component of velocity may not have been measured.

TABLE II

SAMPLE TABULATION

WALLOPS SMOKE-TRAIL TEST NO. LRC 009 LAUNCHED APR 06 1961 1435 EST DELTA Z 25 METERS DELTA T 60 SECONDS

MIONA RIGHT FRAMES 7 AND 17 BATTLE POINT RIGHT FRAMES 7 AND 17

Z (METERS)	VX (MPS)	VY (MPS)	V (MPS)	THETA (DEGREES)	SHEAR X (/SEC)	SHEAR Y (/SEC)	SHEAR V (/SEC)	SHEAR M (/SEC)
10075	79.4	10.6	80.10	262.59	.024	-.024	.033	.020
10100	80.2	10.0	80.82	263.15	.032	-.024	.039	.028
10125	80.7	9.4	81.25	263.72	.020	-.024	.031	.017
10150	81.2	8.7	81.66	264.29	.020	-.028	.034	.016
10175	81.7	8.1	82.10	264.86	.020	-.024	.031	.017
10200	82.2	7.3	82.52	265.43	.020	-.032	.037	.016
10225	82.5	6.4	82.75	266.00	.012	-.036	.037	.009
10250	82.8	5.5	82.98	266.57	.012	-.036	.037	.009
10275	83.2	5.1	83.36	266.57	.016	-.016	.022	.015
10300	83.7	4.7	83.83	267.14	.020	-.016	.025	.018
10325	84.2	4.5	84.32	267.14	.020	-.008	.021	.019
10350	84.6	4.4	84.71	267.14	.016	-.004	.016	.015
10375	85.2	4.0	85.29	267.71	.024	-.016	.028	.023
10400	85.7	3.1	85.76	268.29	.020	-.036	.041	.018
10425	86.2	2.4	86.23	268.86	.020	-.028	.034	.018
10450	86.7	1.9	86.72	268.86	.020	-.020	.028	.019
10475	87.2	1.5	87.21	269.43	.020	-.016	.025	.019
10500	87.6	.9	87.60	269.43	.016	-.024	.028	.015
10525	88.0	.5	88.00	270.00	.016	-.016	.022	.016
10550	88.1	.4	88.10	270.00	.004	-.004	.005	.004
10575	88.6	1.2	88.61	269.43	.020	.032	.037	.020
10600	88.9	1.6	88.91	269.43	.012	.016	.019	.012
10625	89.1	1.6	89.11	269.43	.008	.000	.007	.008
10650	89.4	1.7	89.42	269.43	.012	.004	.012	.012
10675	89.7	1.6	89.71	269.43	.012	-.004	.012	.011
10700	89.9	1.7	89.92	269.43	.008	.004	.008	.008
10725	90.0	1.8	90.02	268.86	.004	.004	.005	.004
10750	90.3	1.6	90.31	269.43	.012	-.008	.014	.011
10775	90.2	1.6	90.21	269.43	-.004	.000	.003	.004
10800	90.1	1.6	90.11	269.43	-.004	.000	.003	.004
10825	90.4	1.8	90.42	269.43	.012	.008	.014	.012
10850	90.9	2.3	90.93	268.86	.020	.020	.028	.020
10875	91.6	2.9	91.65	268.29	.028	.024	.036	.028
10900	91.9	2.9	91.95	268.29	.012	.000	.012	.012
10925	92.2	2.9	92.25	268.29	.012	.000	.012	.012
10950	92.5	2.8	92.54	268.29	.012	-.004	.012	.011
10975	92.5	2.1	92.52	268.86	.000	-.028	.028	.000
11000	92.6	1.5	92.61	269.43	.004	-.024	.024	.003

Z	Altitude, meters
VX	West-to-east component of velocity, meters per second
VY	South-to-north component of velocity, meters per second
V	Magnitude of resultant velocity, meters per second
Theta	Direction from which wind is blowing, degrees
Shear X	$\delta VX/\delta Z$, per second
Shear Y	$\delta VY/\delta Z$, per second
Shear M	$\delta V/\delta Z$, per second
Shear V	$\sqrt{\left(\frac{\delta VX}{\delta Z}\right)^2 + \left(\frac{\delta VY}{\delta Z}\right)^2}$, per second

TABLE III

ROOT-MEAN-SQUARE VELOCITY ERRORS COMPUTED FROM

INDEPENDENT PAIRS OF PHOTOGRAPHS

Altitude range, km	Root-mean-square velocity errors		
	West-to-east component, m/sec	South-to-north component, m/sec	Vector, m/sec
	Trail 008; time interval, 60 sec		
2.8 to 5	0.4	0.5	0.6
5 to 9	.3	.3	.4
9 to 13	.9	.9	1.3
13 to 18.4	.7	2.1	2.2
2.8 to 18.4	.7	1.3	1.5
	Trail 009; time interval, 60 sec		
2.6 to 5	0.6	1.2	1.3
5 to 9	.1	.3	.3
9 to 13	.5	.5	.7
2.6 to 13	.4	.7	.8
	Trail 009; time interval, 30 sec		
2.8 to 5	0.5	0.7	0.8
5 to 9	.2	.4	.5
9 to 13	.6	.7	.9
2.8 to 13	.5	.6	.8
	Trail 018; time interval, 60 sec		
2.6 to 5	0.1	0.2	0.2
5 to 9	.1	.2	.2
9 to 12.3	.4	.6	.7
2.6 to 12.3	.2	.3	.4
	Trail 021; time interval, 60 sec		
4.5 to 5	0.3	0.3	0.4
5 to 9	.5	.7	.8
9 to 13	1.5	.6	1.7
13 to 16.1	1.3	.7	1.5
4.5 to 16.1	1.2	.6	1.3
	Trail 027; time interval, 60 sec		
5 to 9	0.4	0.5	0.6
9 to 13	1.1	1.2	1.6
13 to 15.3	1.7	1.4	2.2
5 to 15.3	1.1	1.0	1.5

TABLE IV

ROOT-MEAN-SQUARE DIFFERENCES BETWEEN WIND VELOCITIES

DERIVED FROM SIMULTANEOUS SMOKE TRAILS

Altitude range, km	Root-mean-square differences		
	West-to-east component, m/sec	South-to-north component, m/sec	Vector, m/sec
Trails 023 and 024; time interval, 60 sec			
4 to 5	1.1	0.8	1.3
5 to 8.9	.4	1.0	1.1
4 to 8.9	.6	1.0	1.2
Trails 023 and 025; time interval, 60 sec			
4 to 5	0.6	0.3	0.7
5 to 8.9	.6	1.1	1.2
4 to 8.9	.6	1.0	1.1
Trails 024 and 025; time interval, 60 sec			
2.9 to 5	0.9	1.3	1.6
5 to 9	.6	1.0	1.2
9 to 12.3	.5	.6	.7
2.9 to 12.3	.6	1.0	1.2

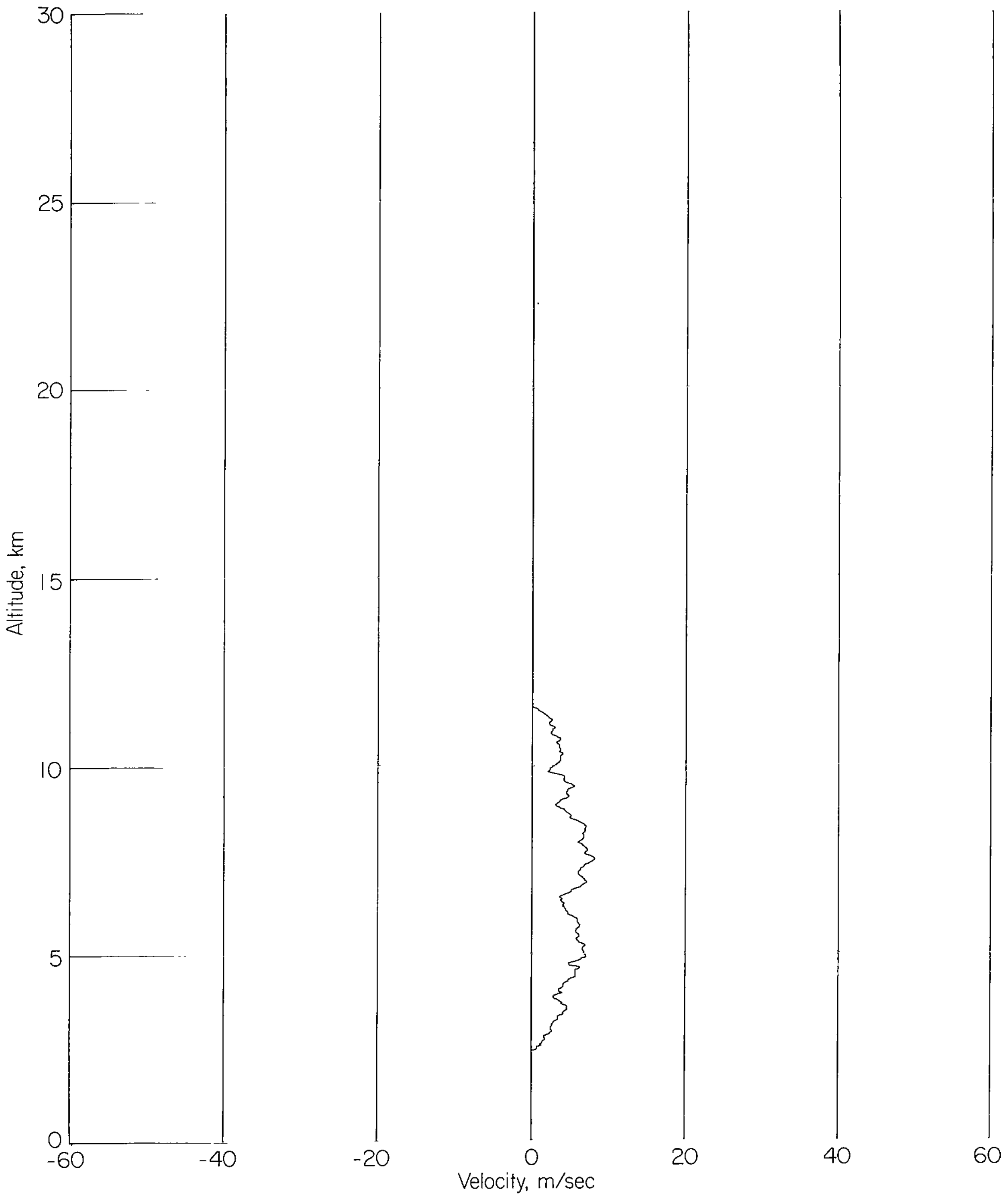

(a) West-to-east velocity component.

Figure 1.- . Smoke-trail wind profile obtained on Sept. 21, 1959. Trail 002; time interval of 30 seconds; height interval of 30 meters.

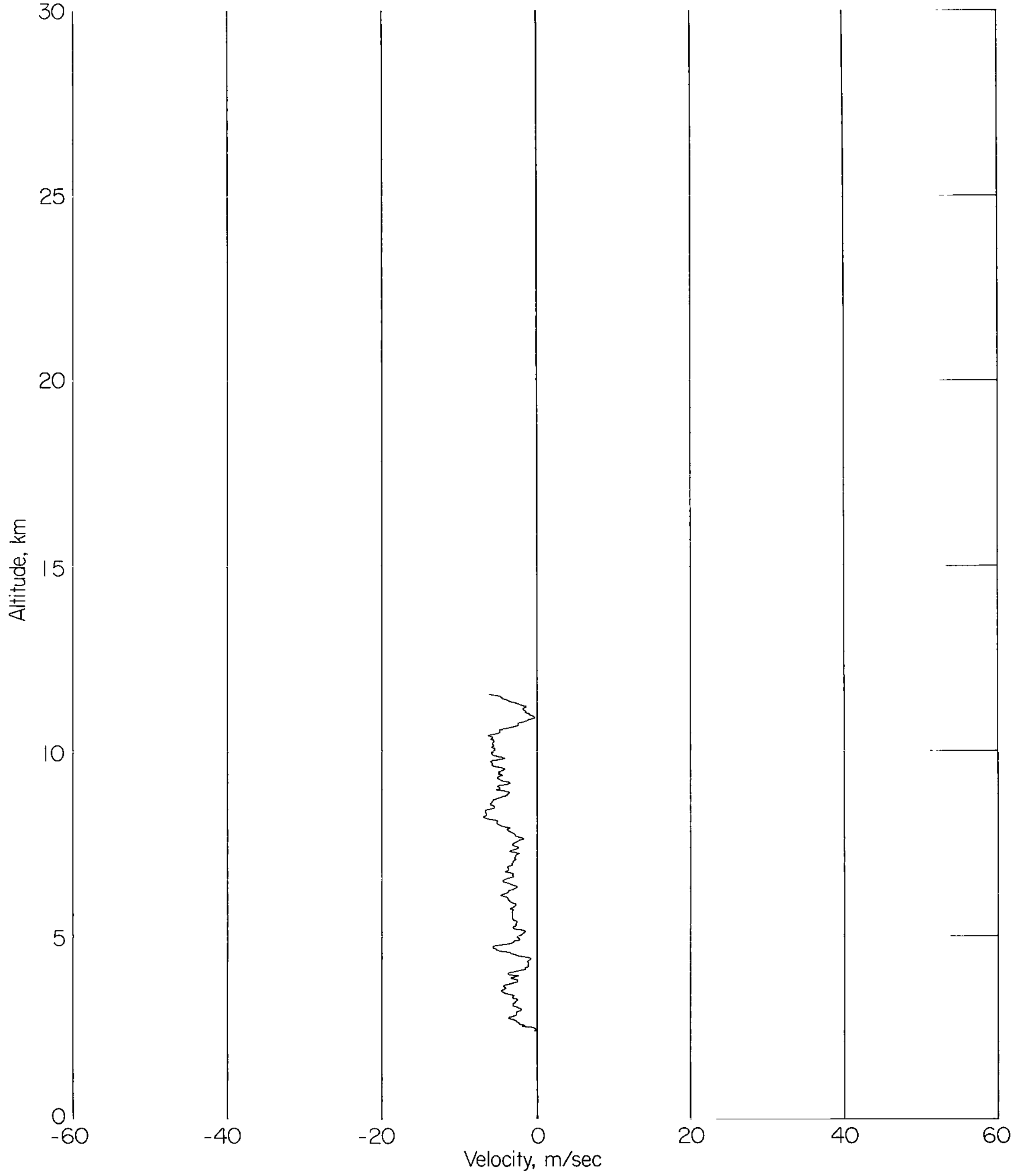

(b) South-to-north velocity component.

Figure 1.- Concluded.

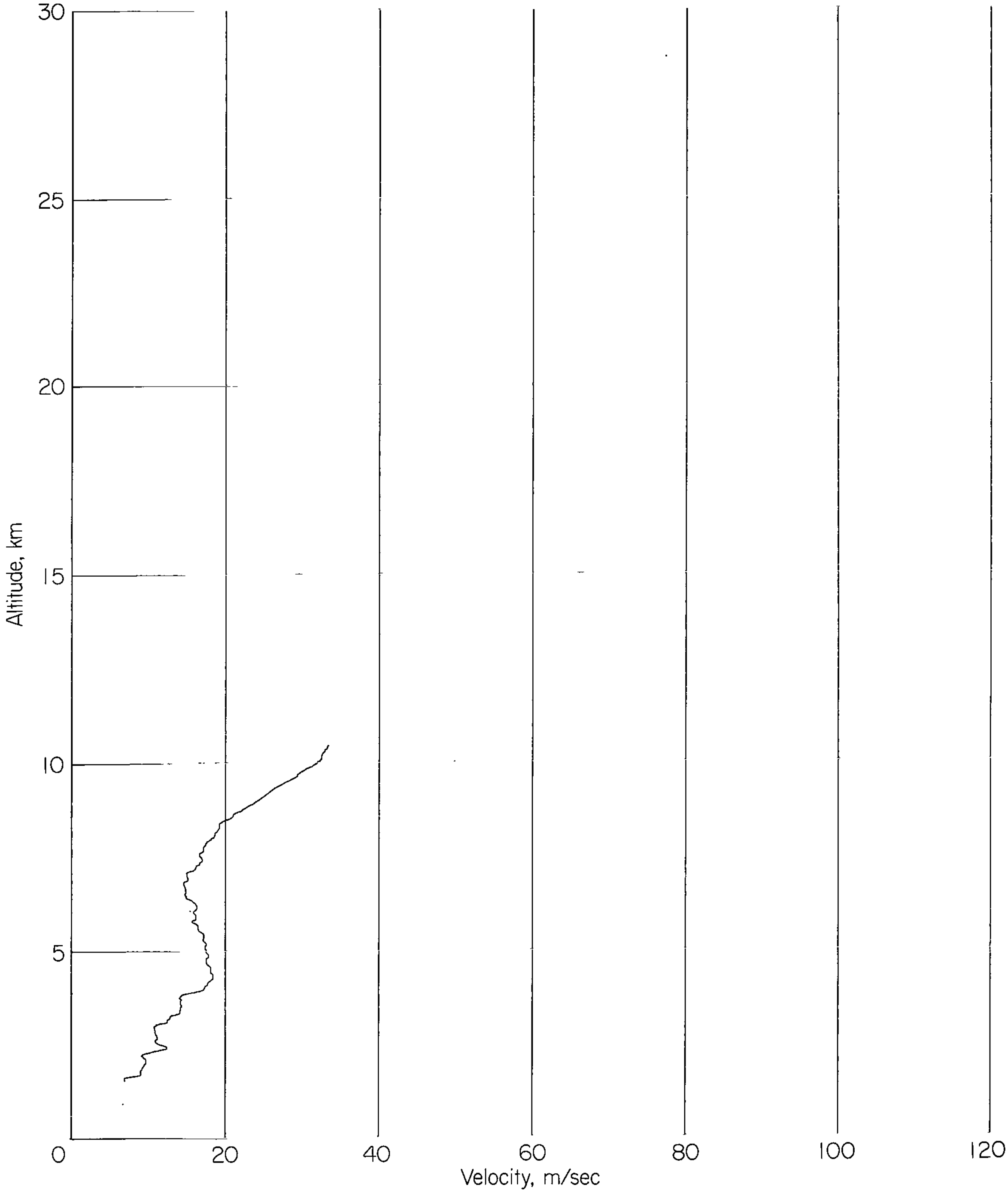

(a) West-to-east velocity component.

Figure 2.- Smoke-trail wind profile obtained on Nov. 4, 1959. Trail 003; time interval of 60 seconds; height interval of 30 meters.

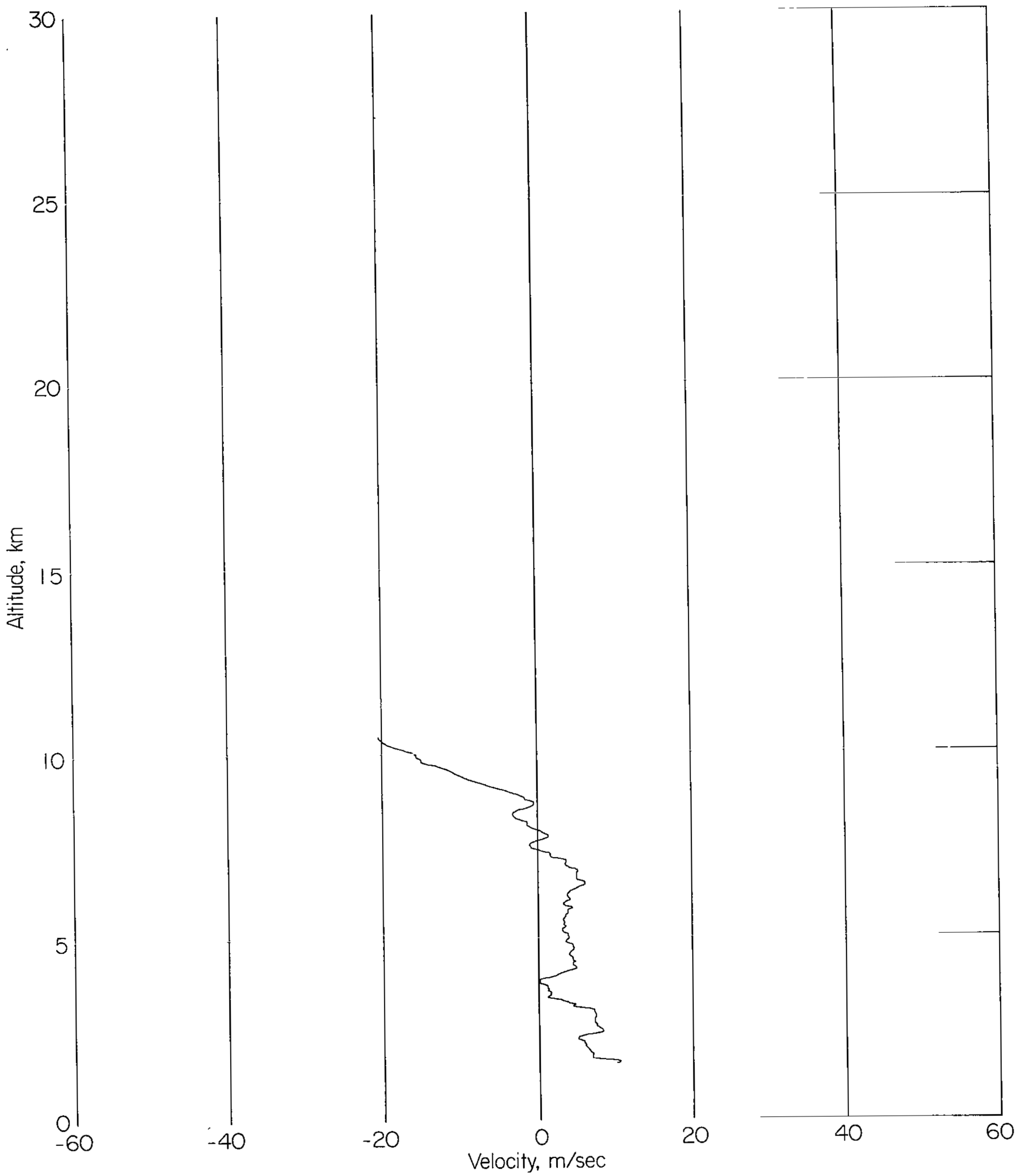

(b) South-to-north velocity component.

Figure 2.- Concluded.

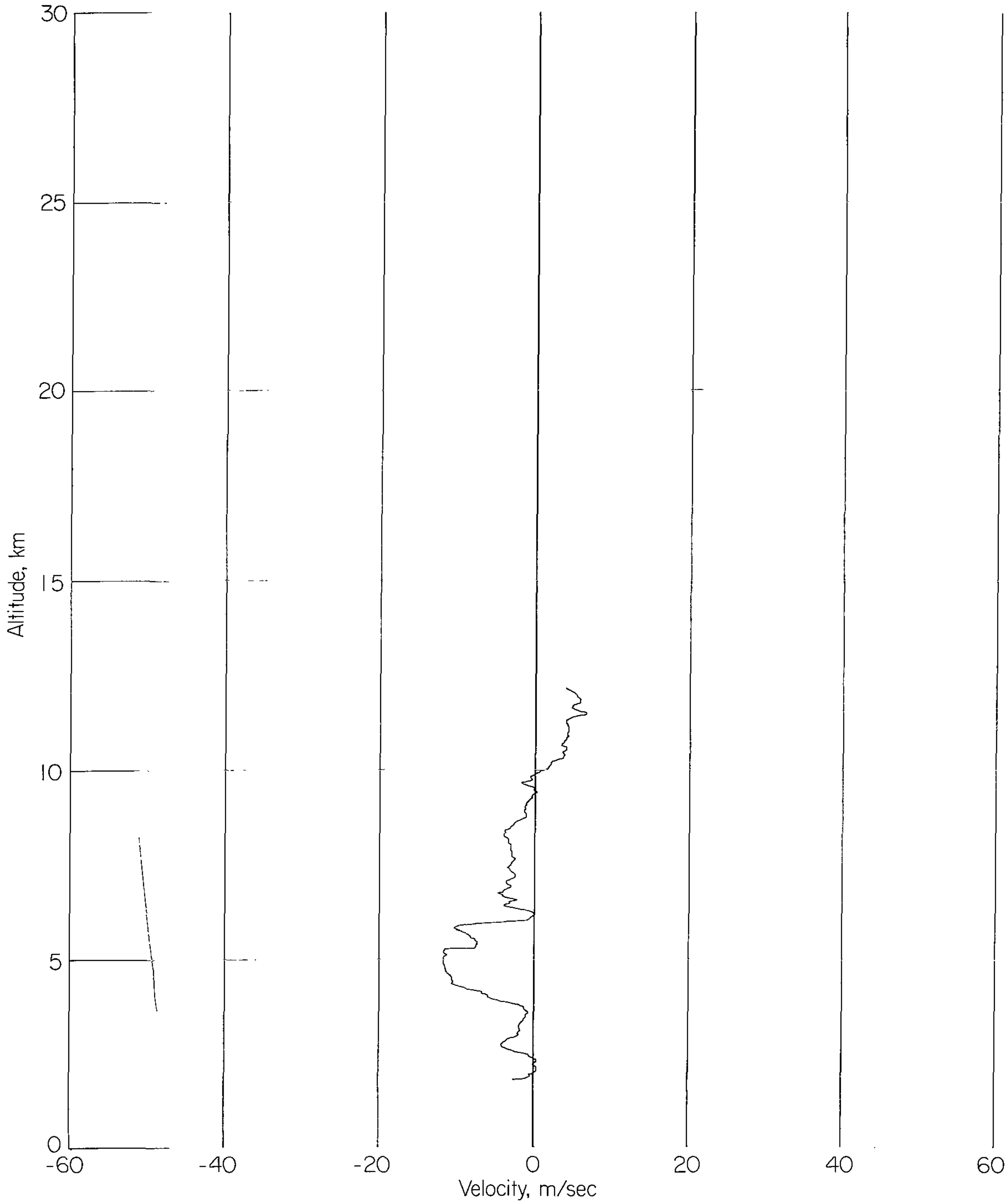

(a) West-to-east velocity component.

Figure 3.- Smoke-trail wind profile obtained on Dec. 4, 1959. Trail 004; time interval of 60 seconds; height interval varied.

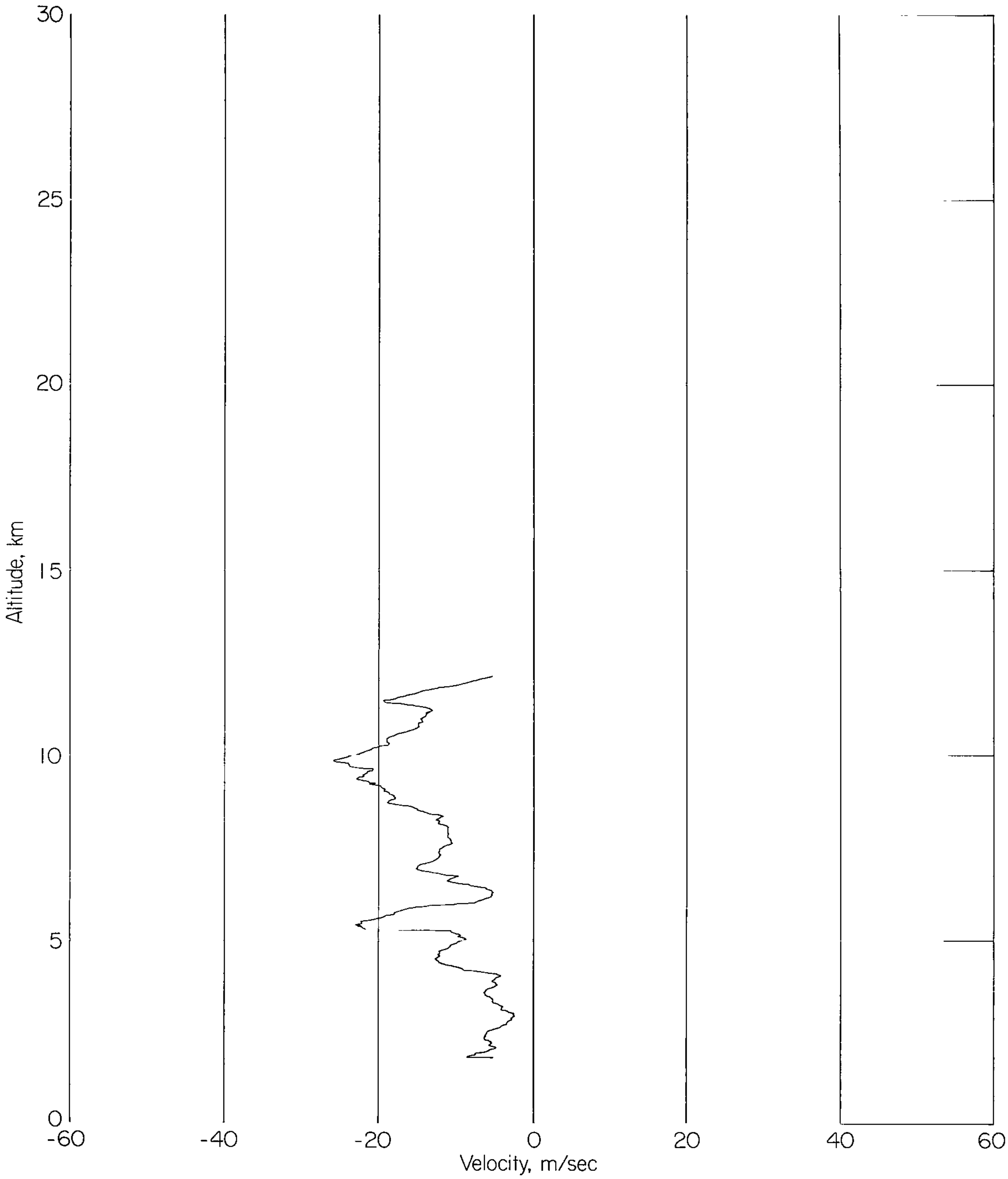

(b) South-to-north velocity component.

Figure 3.- Concluded.

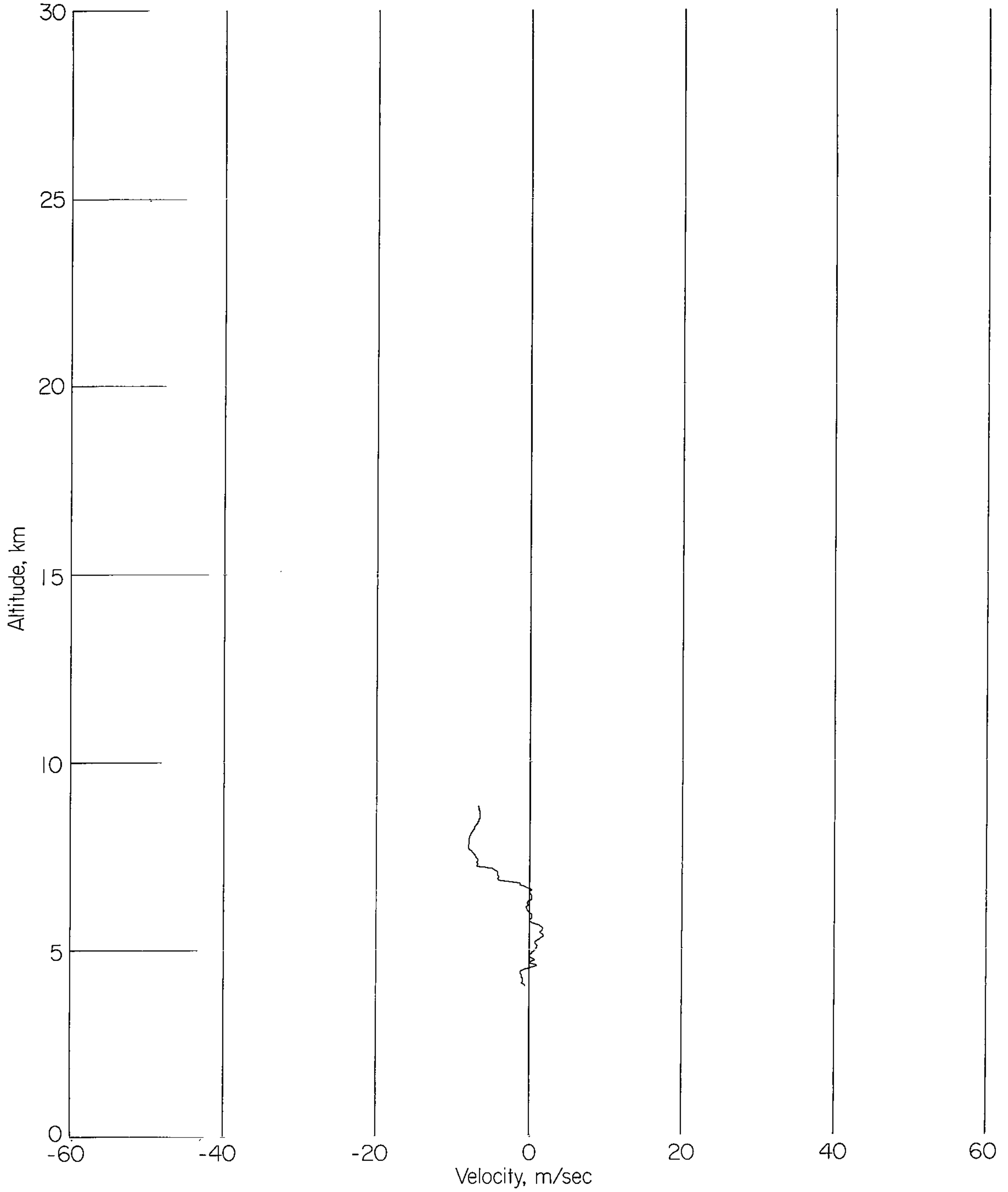

(a) West-to-east velocity component.

Figure 4.- Smoke-trail wind profile obtained on Sept. 8, 1960. Trail 005; time interval of 60 seconds; height interval of 25 meters.

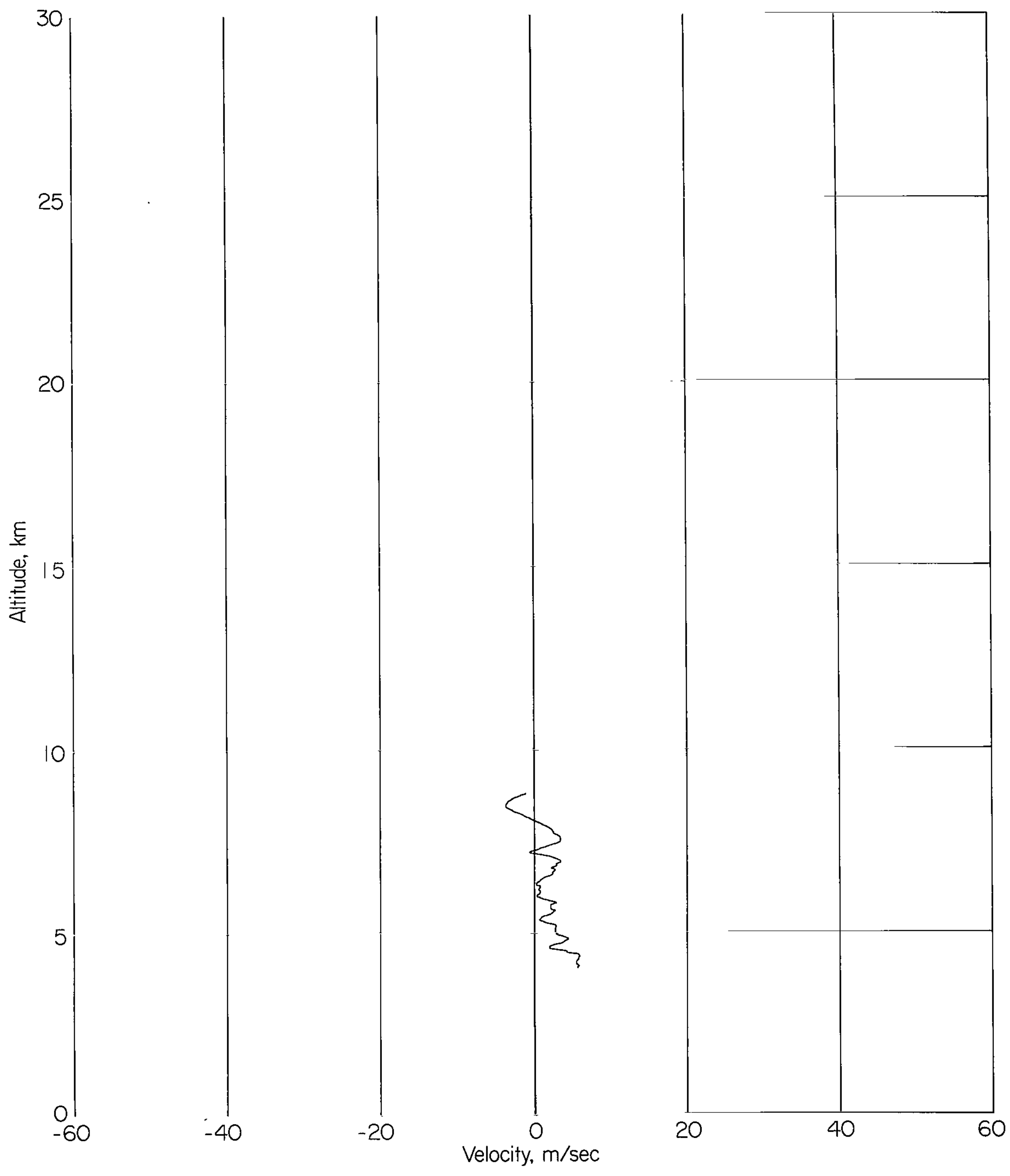

(b) South-to-north velocity component.

Figure 4.- Concluded.

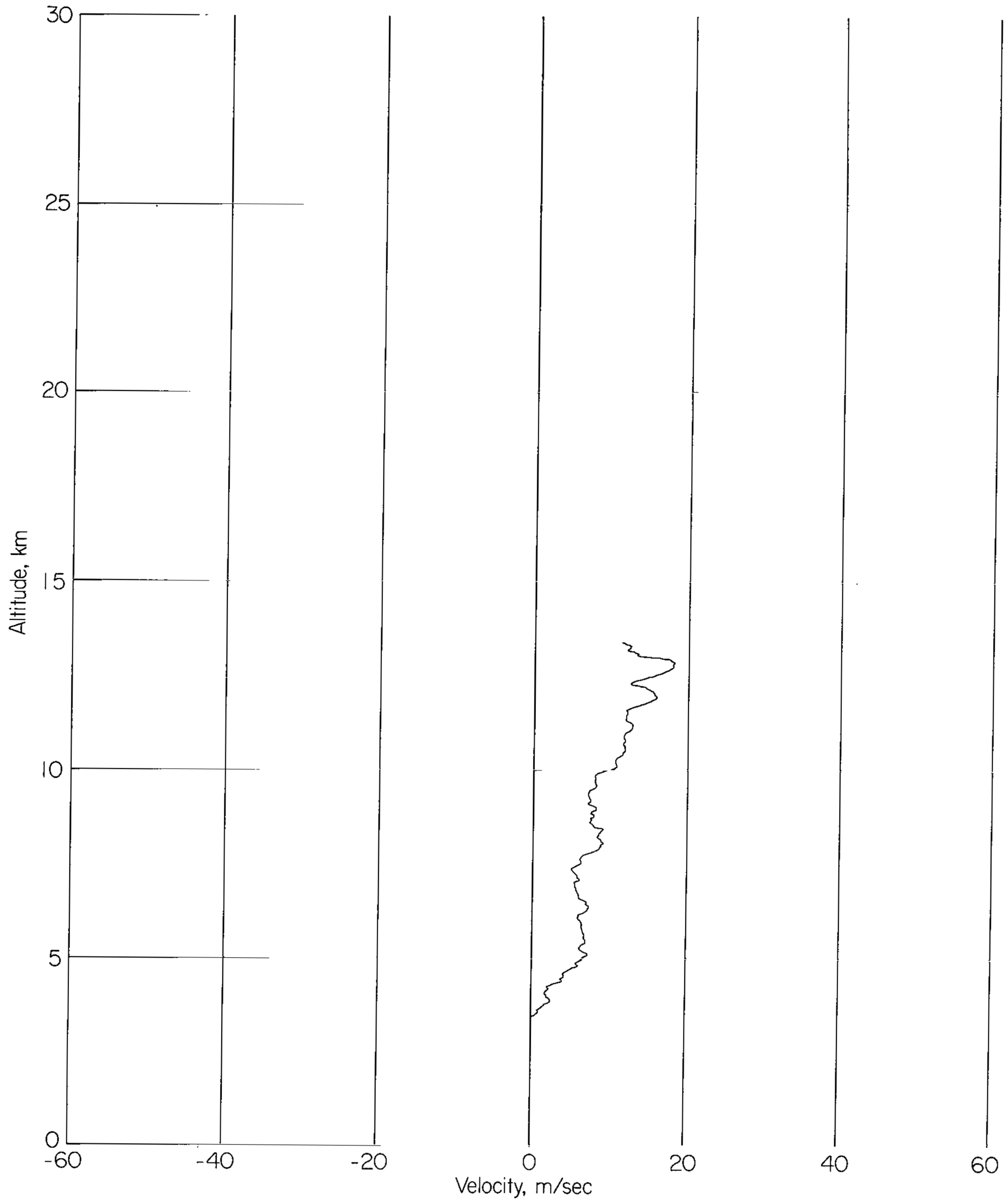

(a) West-to-east velocity component.

Figure 5.- Smoke-trail wind profile obtained on Sept. 23, 1960. Trail 006; time interval of 60 seconds; height interval of 25 meters.

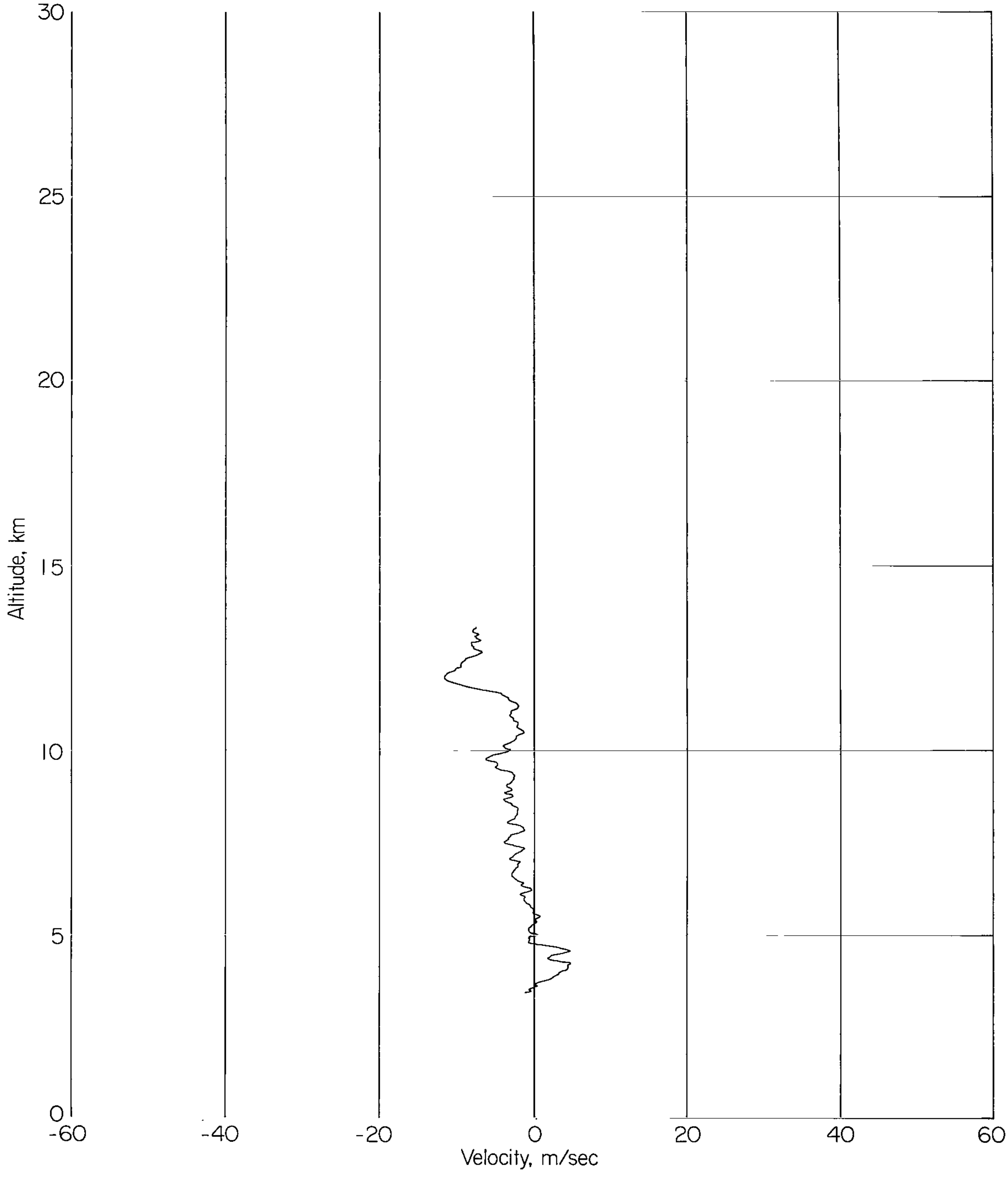

(b) South-to-north velocity component.

Figure 5.- Concluded.

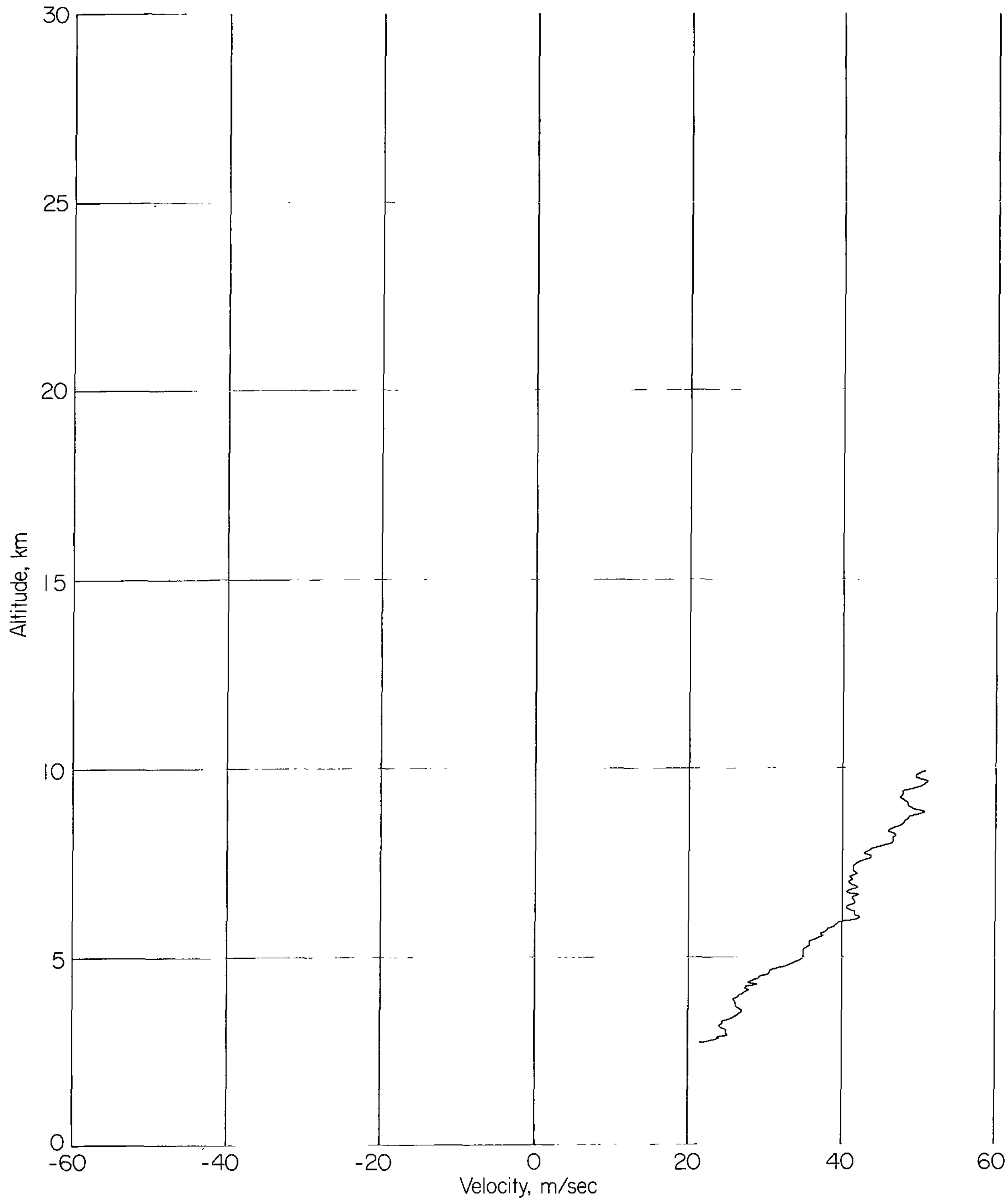

(a) West-to-east velocity component.

Figure 6.- Smoke-trail wind profile obtained on Feb. 15, 1961. Trail 007; time interval of 60 seconds; height interval of 25 meters.

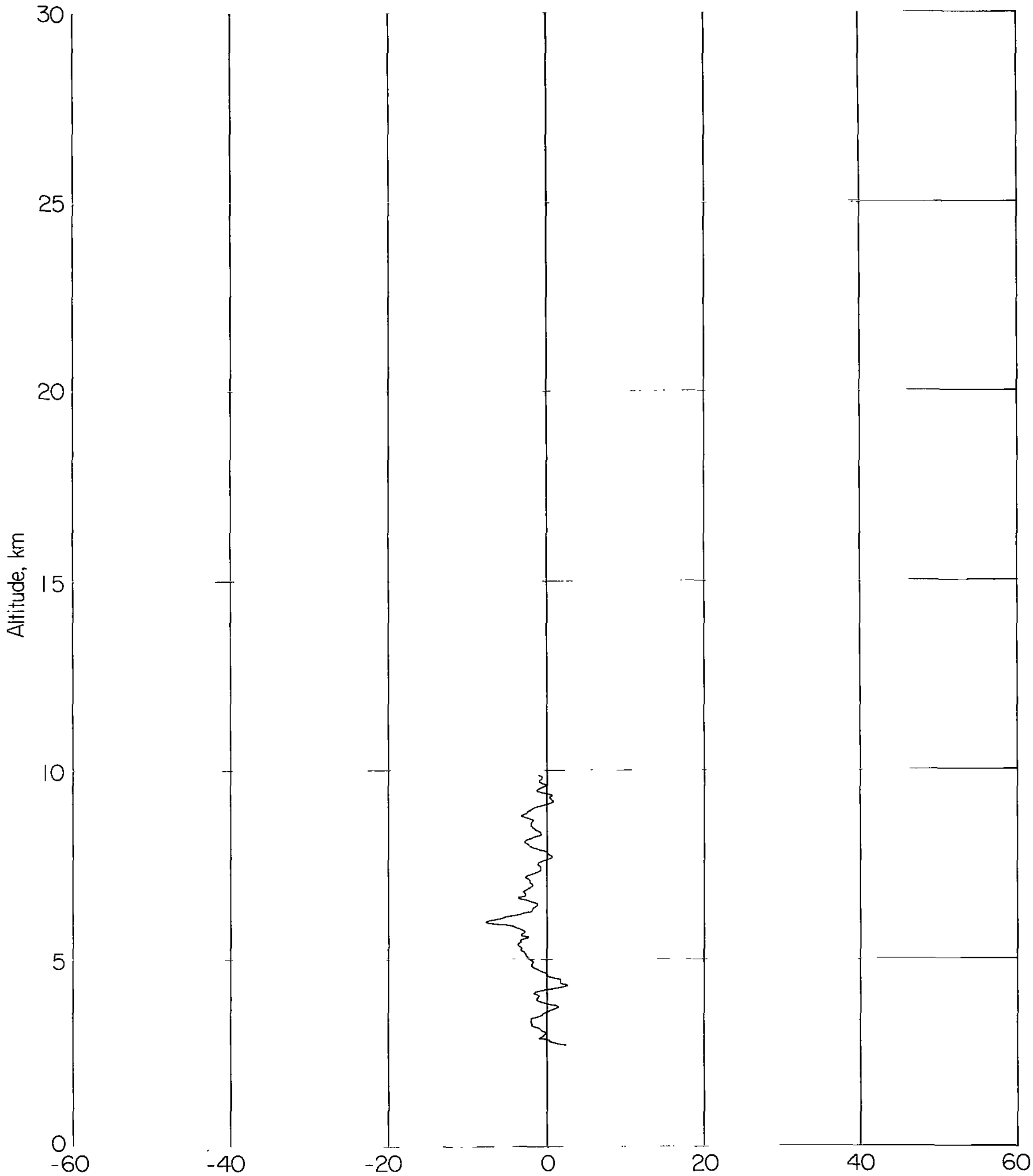

(b) South-to-north velocity components.

Figure 6.- Concluded.

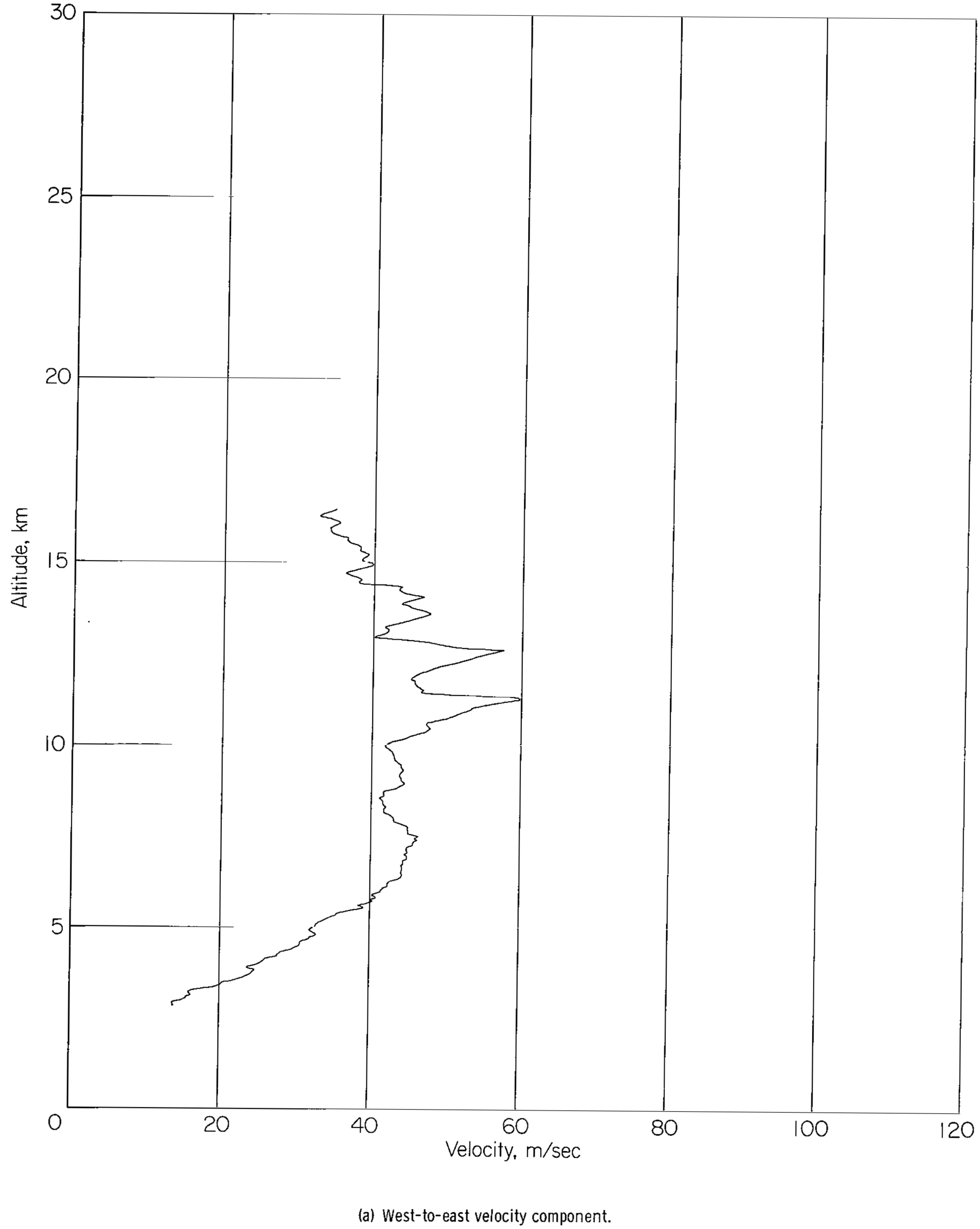

(a) West-to-east velocity component.

Figure 7.- Smoke-trail wind profile obtained on Feb. 16, 1961. Trail 008; time interval of 60 seconds; height interval of 25 meters.

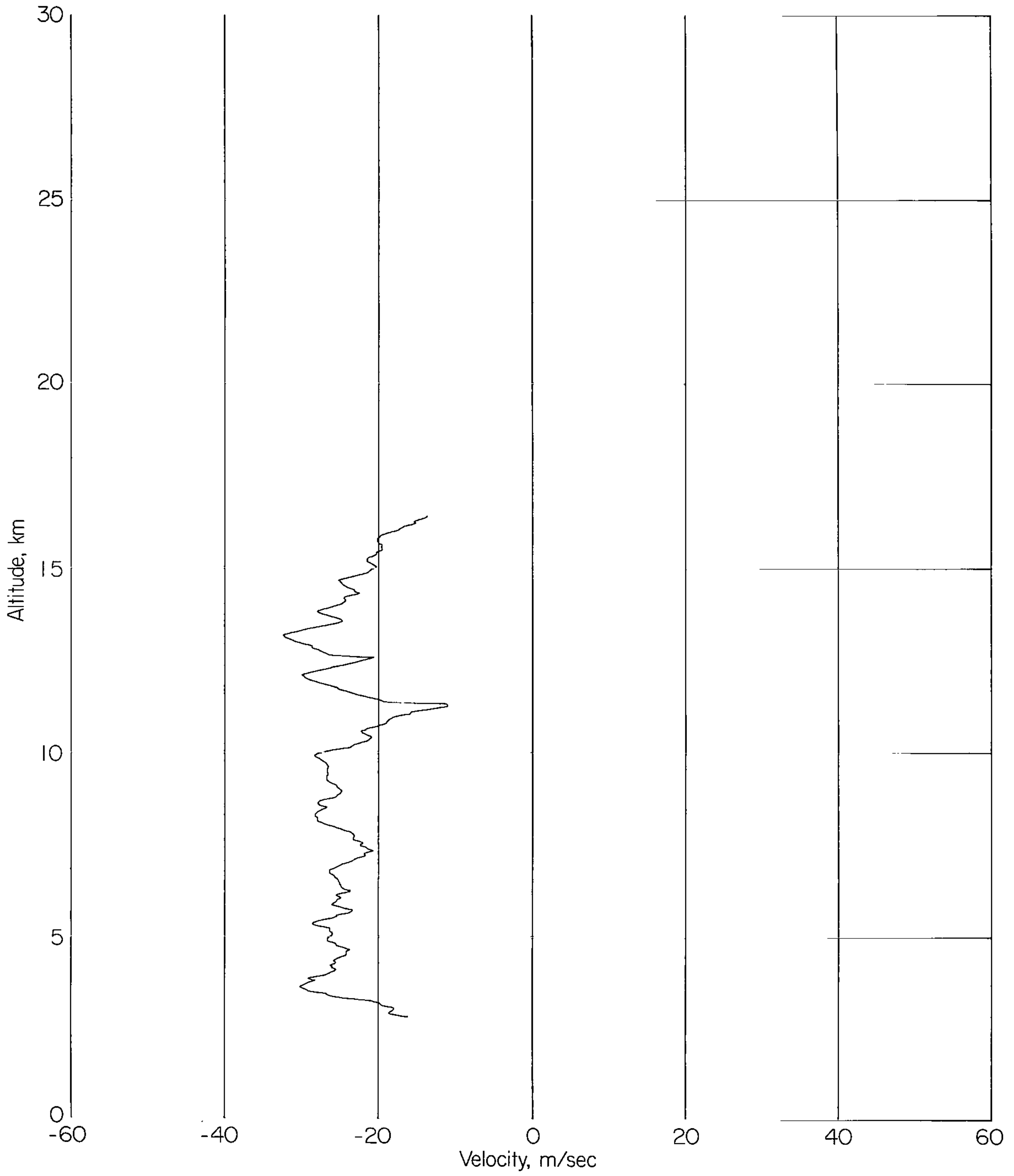

(b) South-to-north velocity component.

Figure 7.- Concluded.

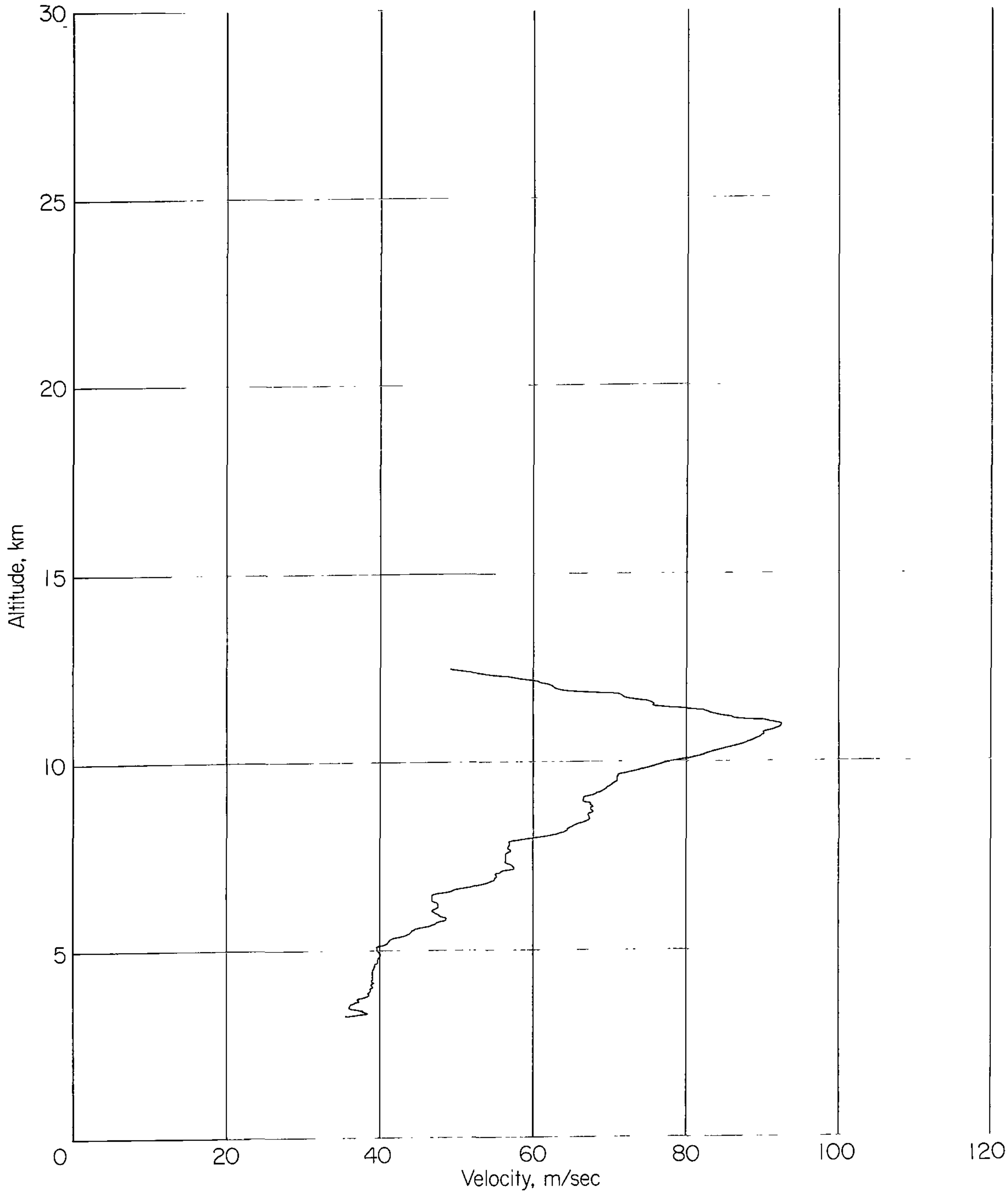

(a) West-to-east velocity component.

Figure 8.- Smoke-trail wind profile obtained on April 6, 1961. Trail 009; time interval of 60 seconds; height interval of 25 meters.

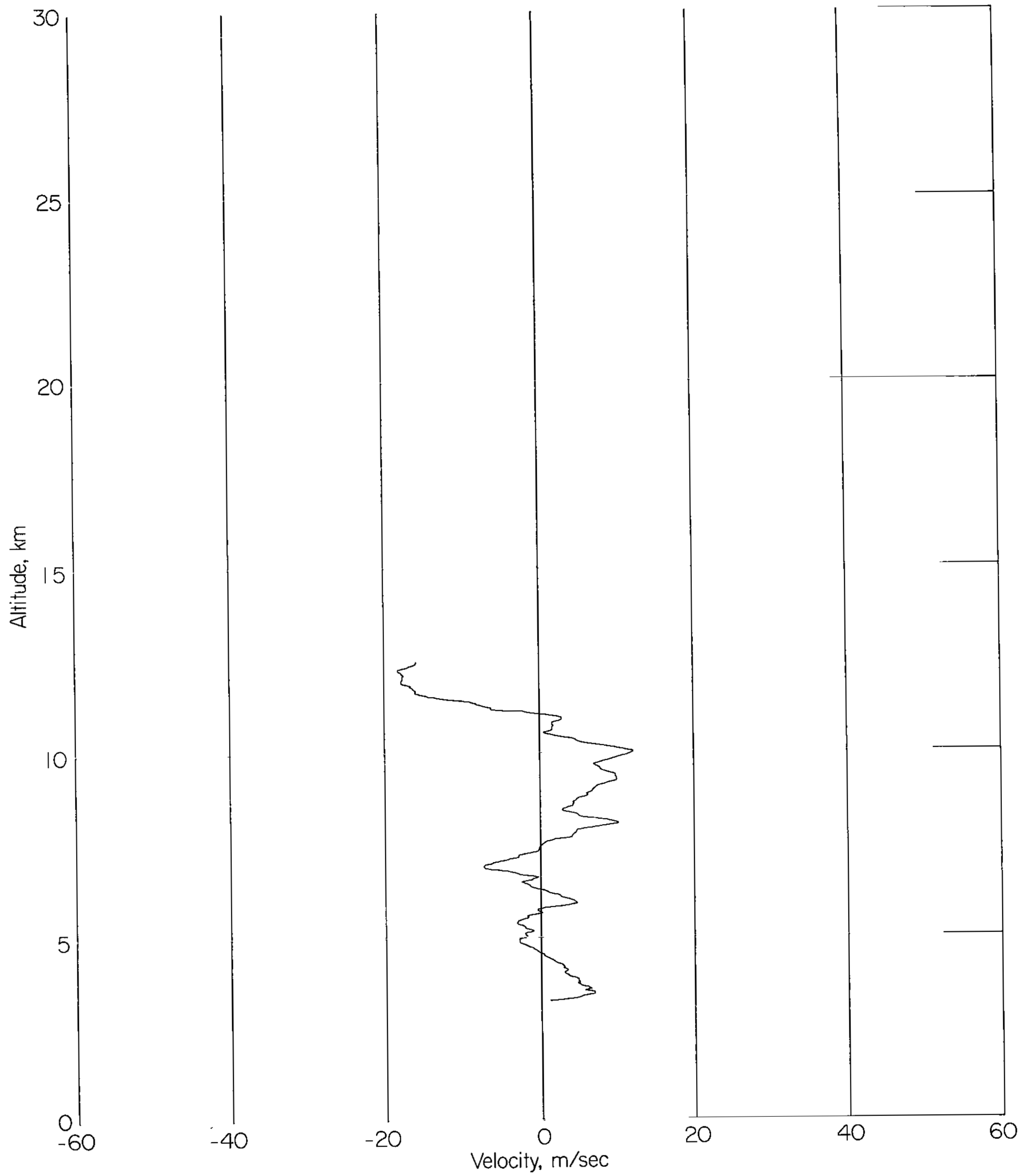

(b) South-to-north velocity component.

Figure 8.- Concluded.

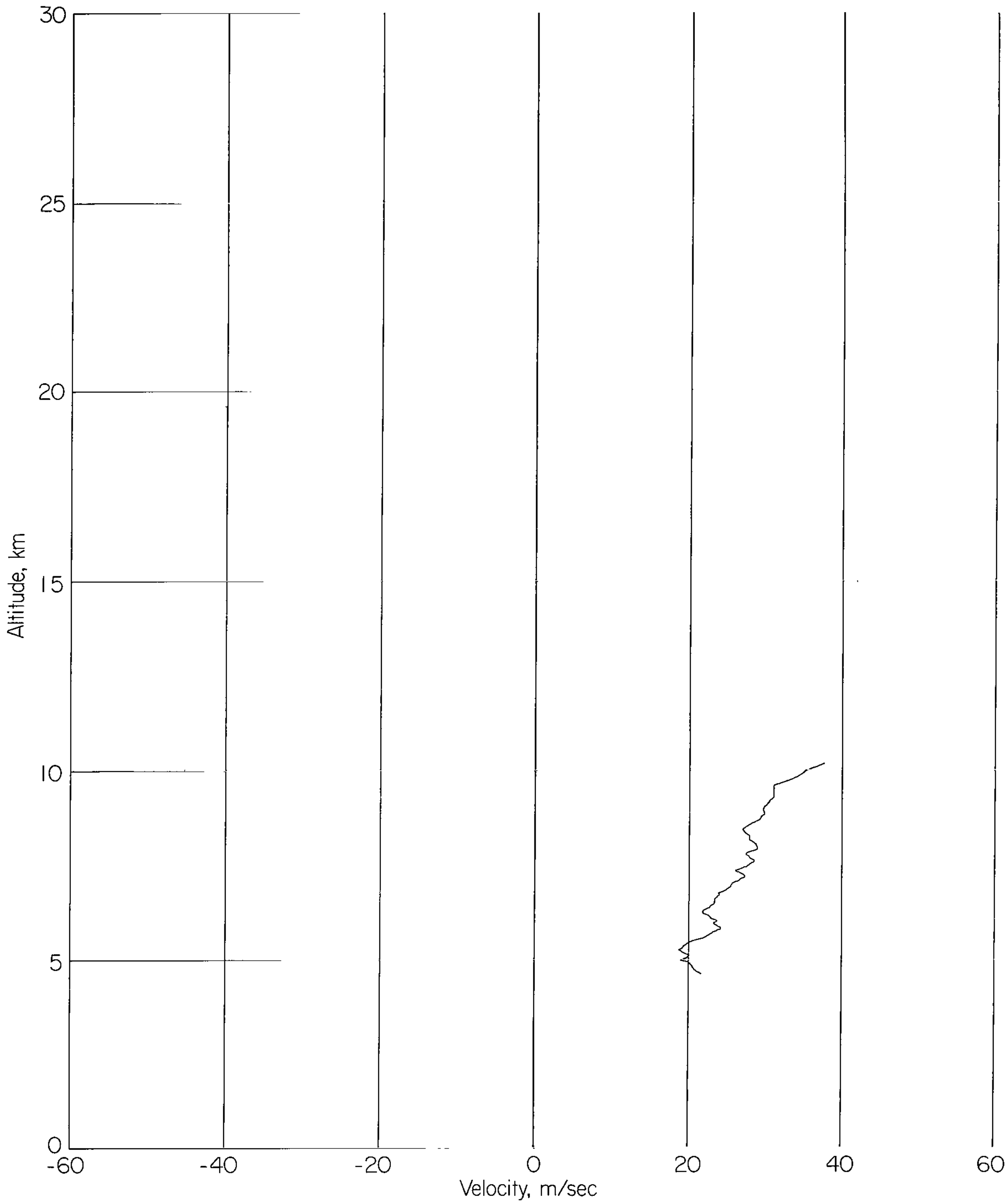

(a) West-to-east velocity component.

Figure 9.- Smoke-trail wind profile obtained on April 14, 1961. Trail 010; time interval of 60 seconds; height interval of 25 meters.

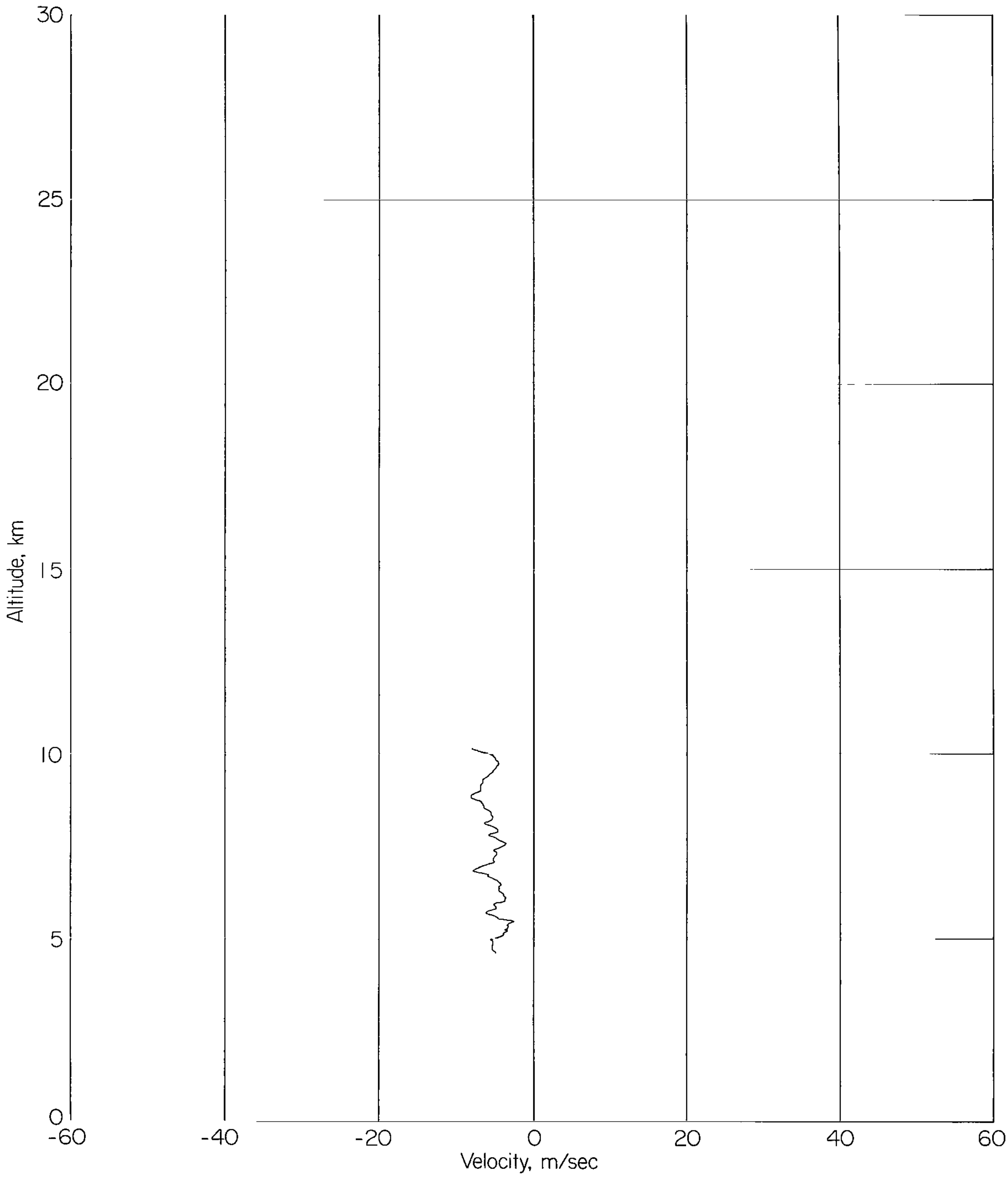

(b) South-to-north velocity component.

Figure 9.- Concluded.

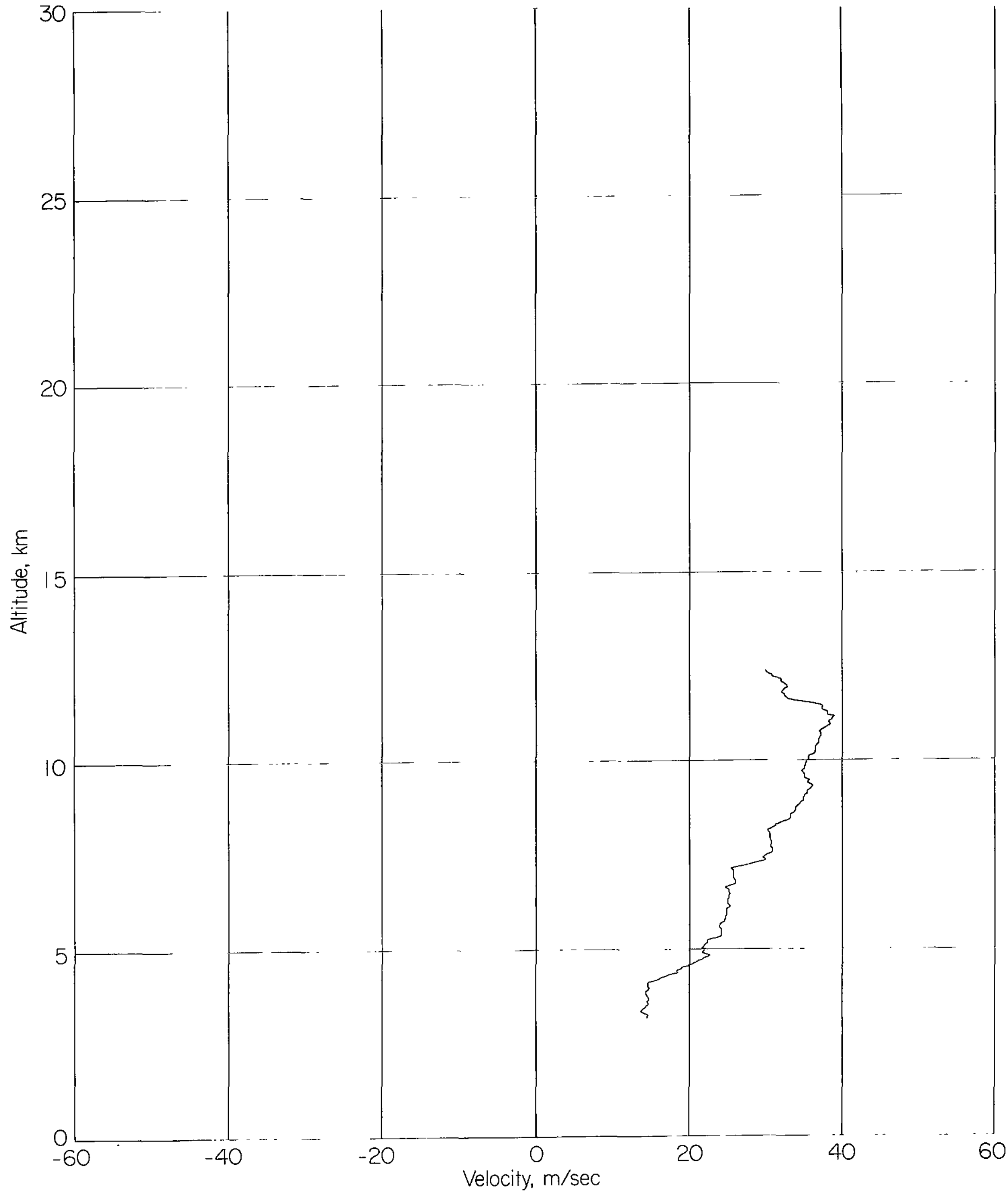

(a) West-to-east velocity component.

Figure 10.- Smoke-trail wind profile obtained on April 14, 1961. Trail 012; time interval of 60 seconds; height interval of 25 meters.

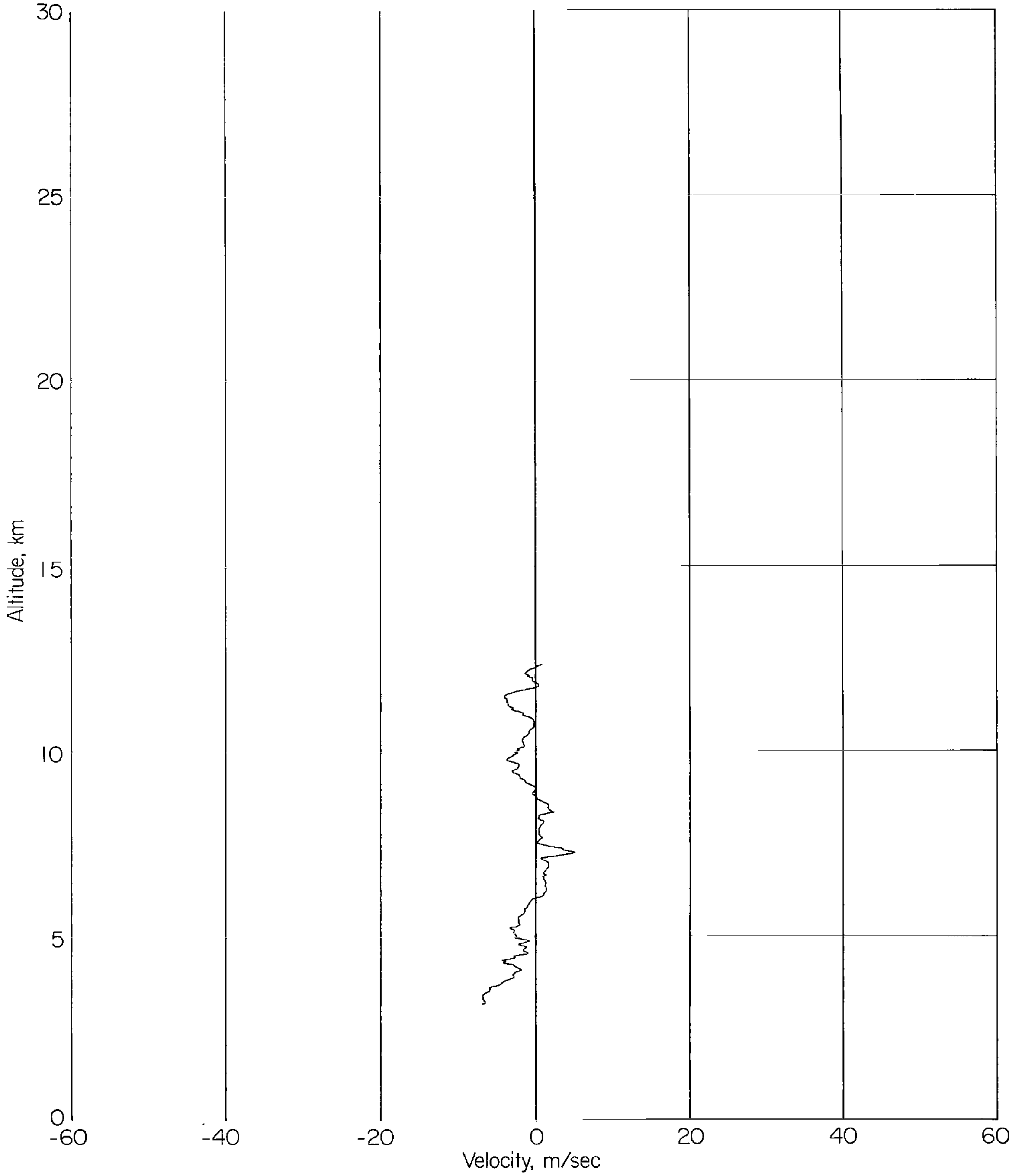

(b) South-to-north velocity component.

Figure 10.- Concluded.

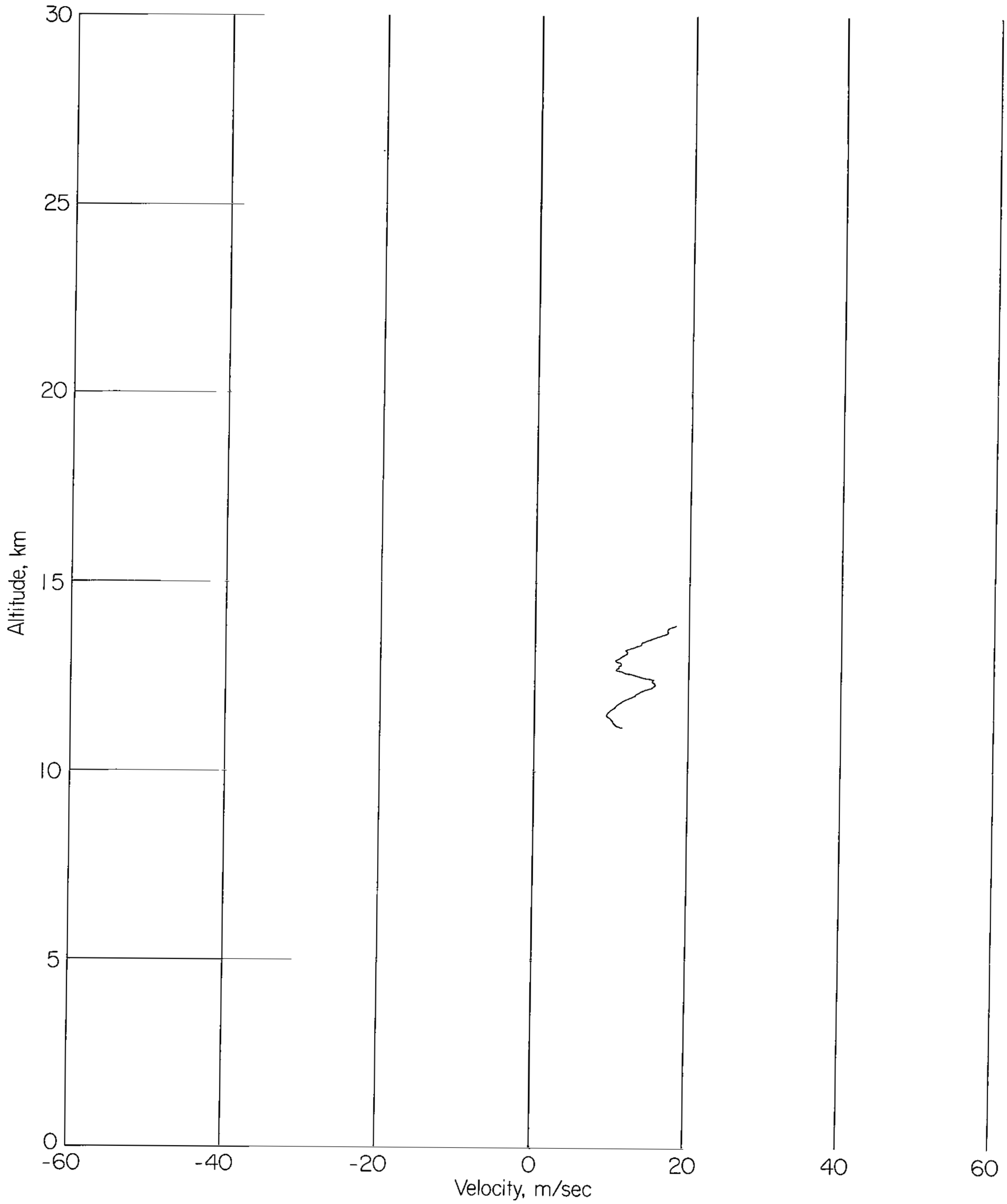

(a) West-to-east velocity component.

Figure 11.- Smoke-trail wind profile obtained on July 14, 1961. Trail 014; time interval of 60 seconds; height interval of 25 meters.

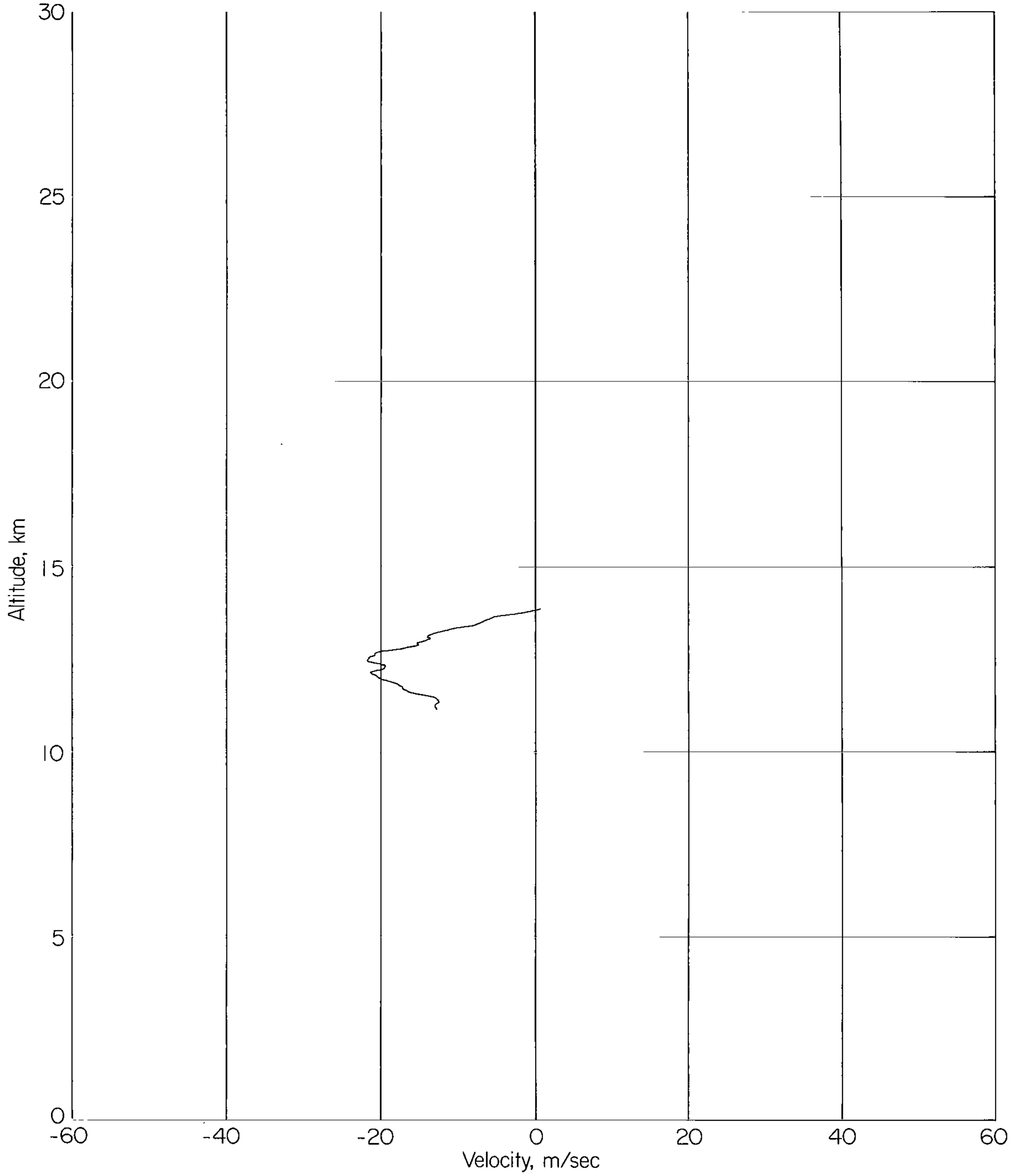

(b) South-to-north velocity component.

Figure 11.- Concluded.

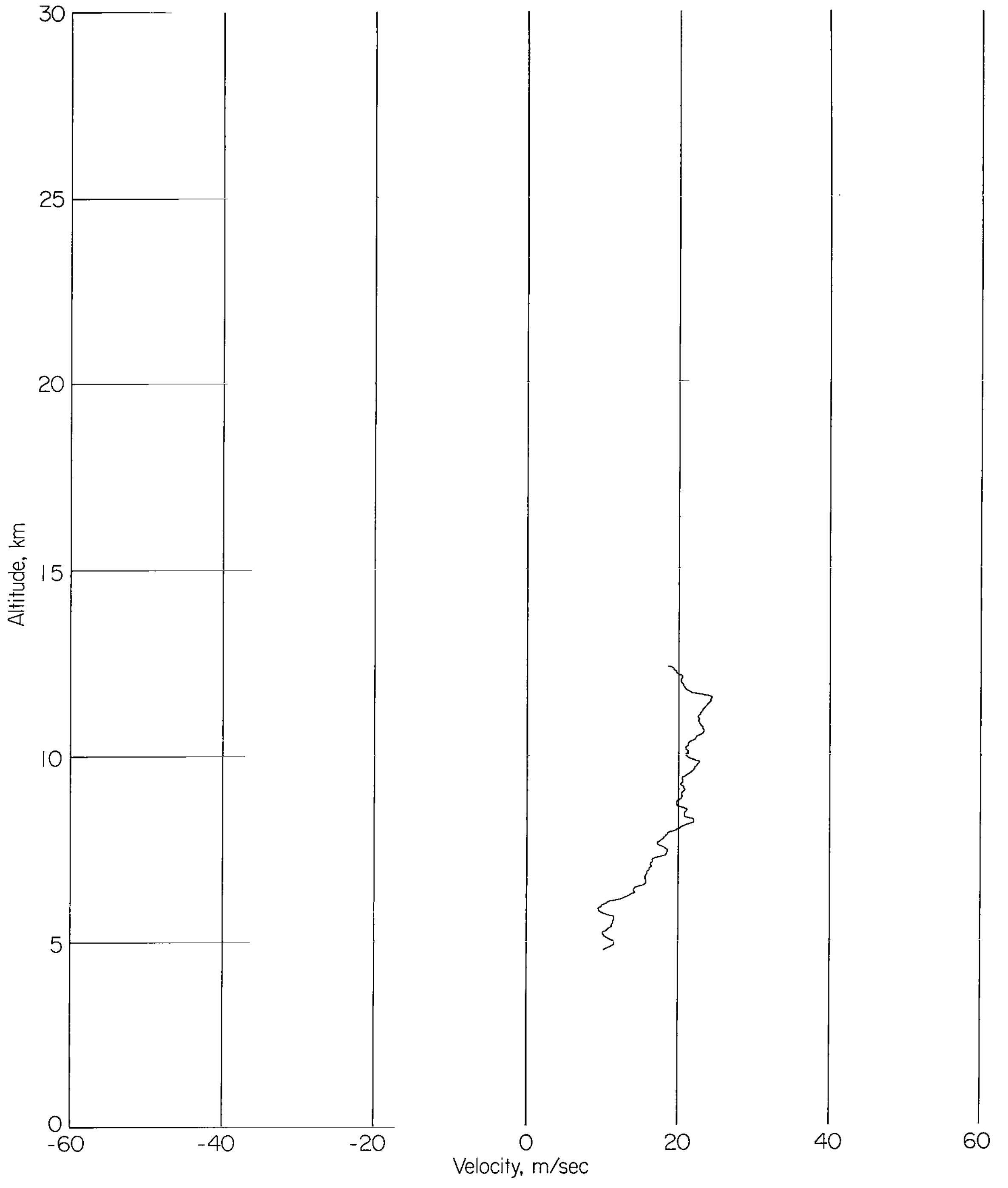

(a) West-to-east velocity component.

Figure 12.- Smoke-trail wind profile obtained on July 14, 1961. Trail 015; time interval of 60 seconds; height interval of 25 meters.

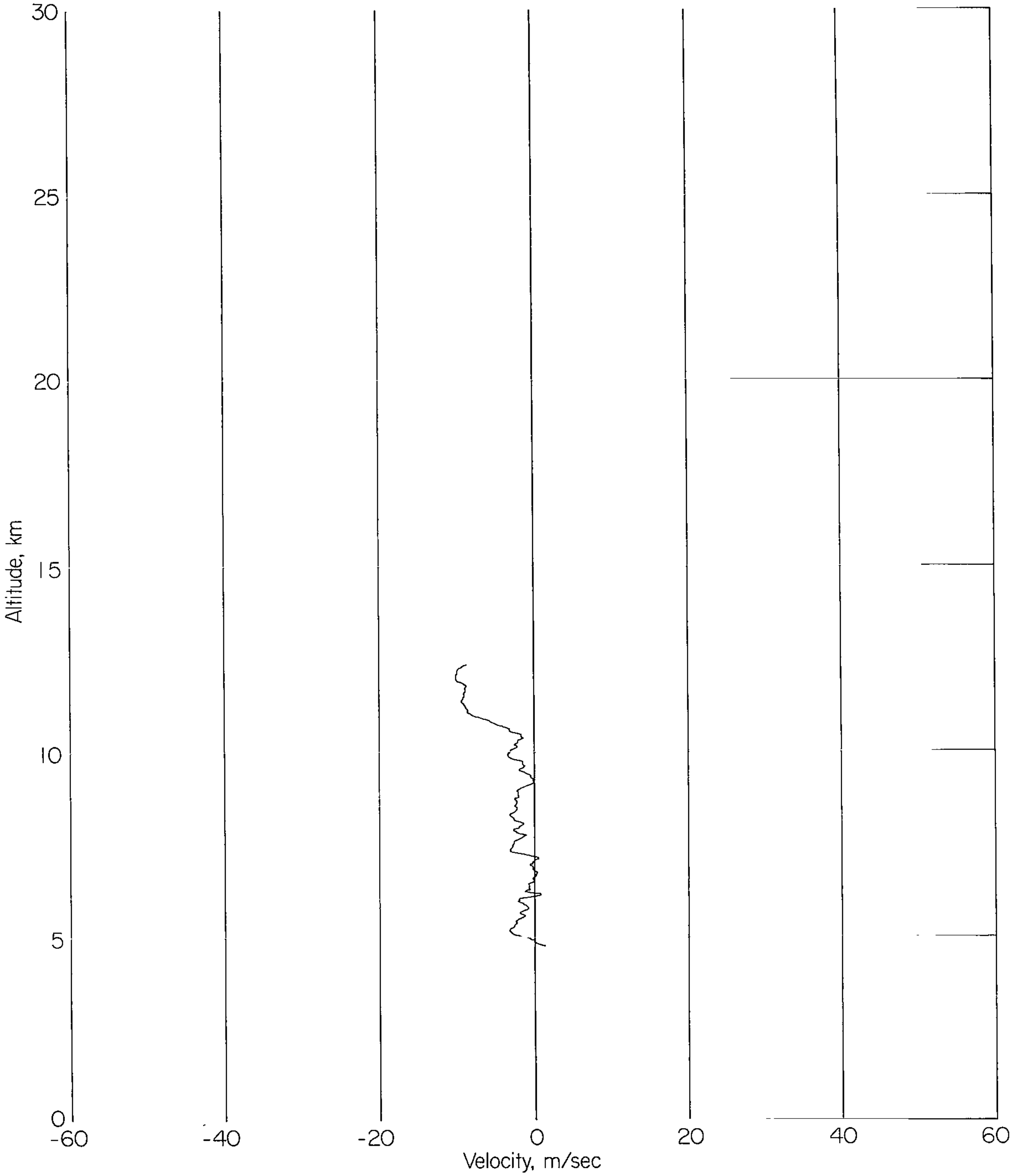

(b) South-to-north velocity component.

Figure 12.- Concluded.

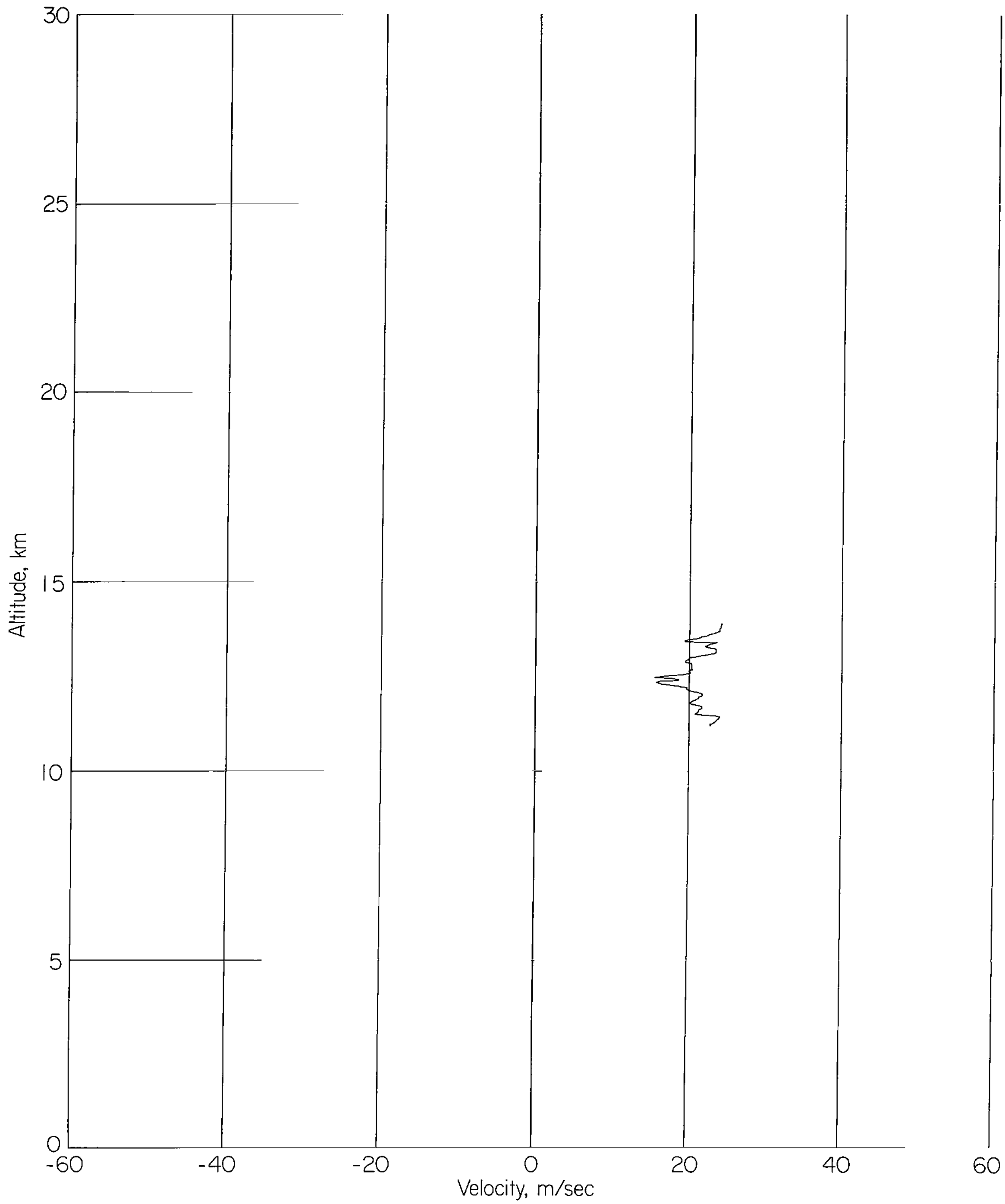

(a) West-to-east velocity component.

Figure 13.- Smoke-trail wind profile obtained on July 14, 1961. Trail 016; time interval of 60 seconds; height interval of 25 meters.

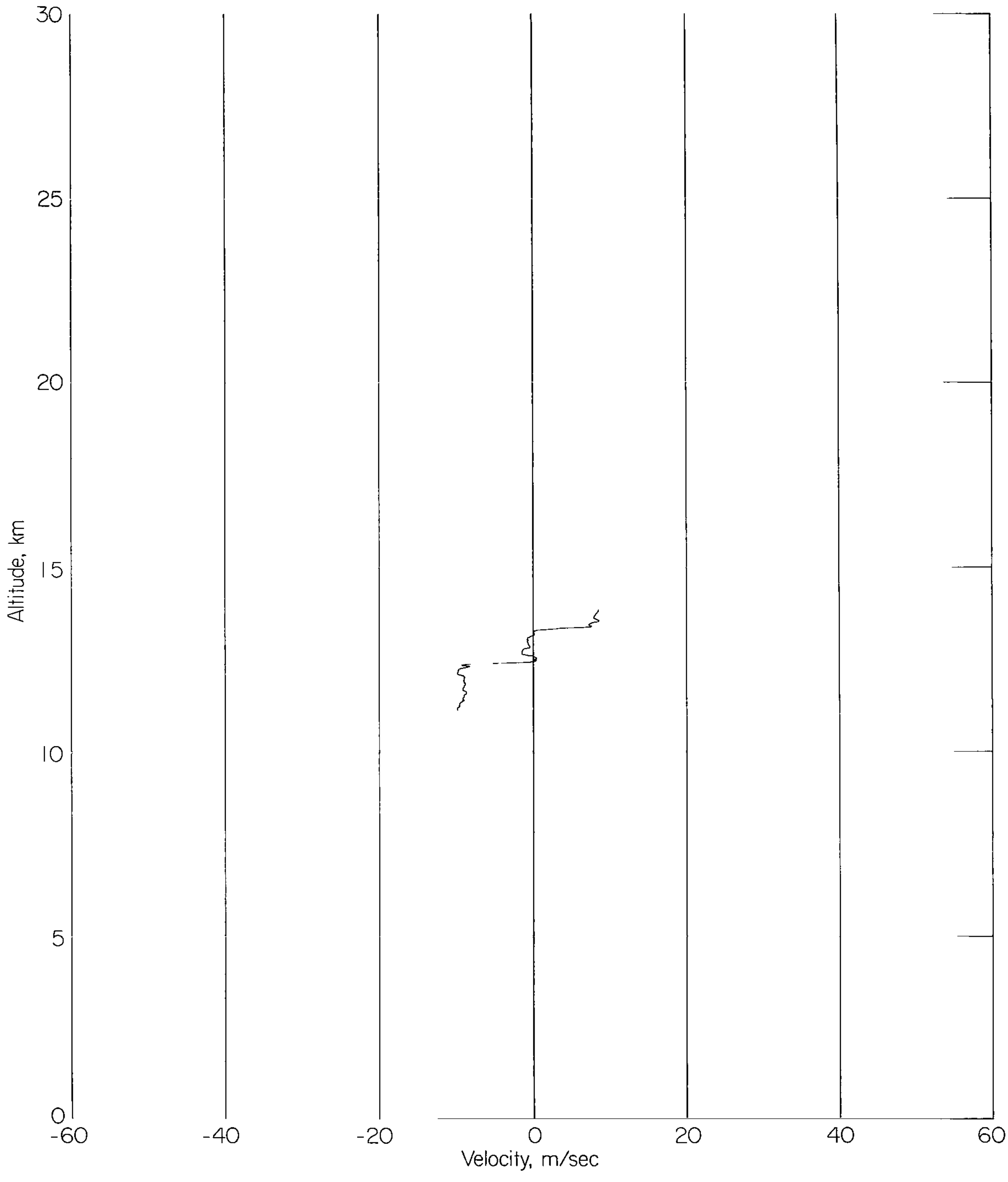

(b) South-to-north velocity component.

Figure 13.- Concluded.

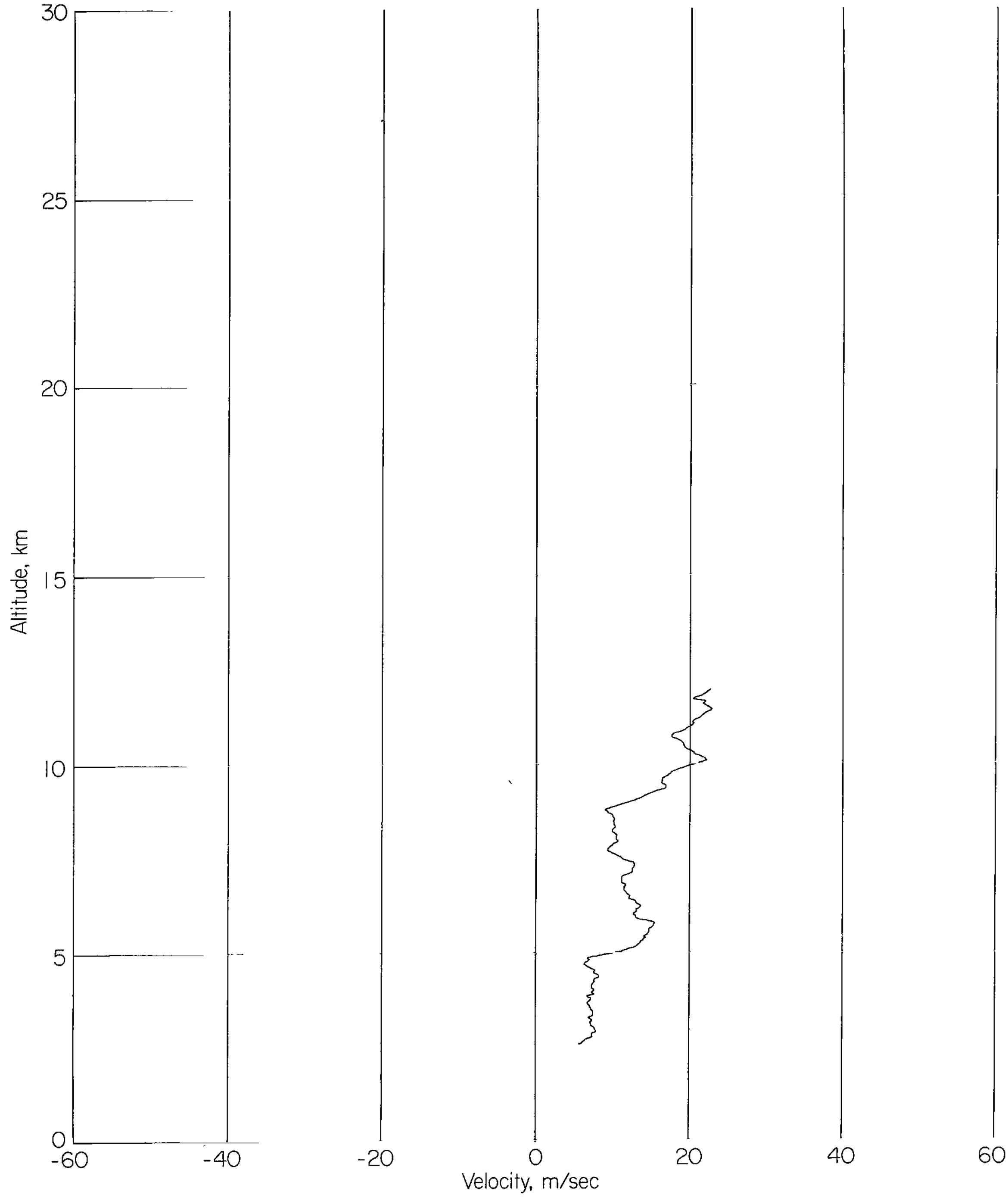

(a) West-to-east velocity component.

Figure 14.- Smoke-trail wind profile obtained on Oct. 24, 1961. Trail 018; time interval of 60 seconds; height interval of 25 meters.

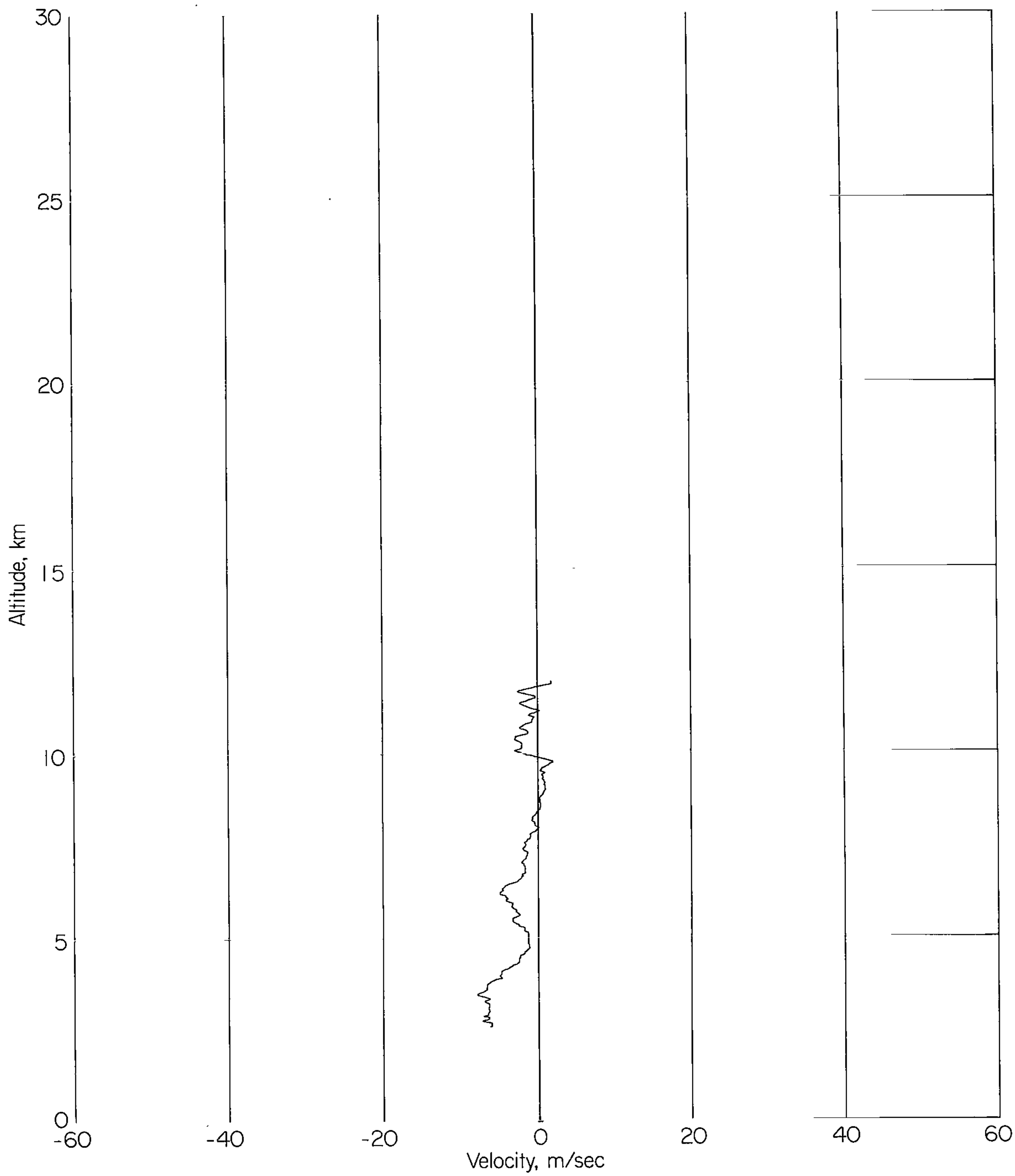

(b) South-to-north velocity component.

Figure 14.- Concluded.

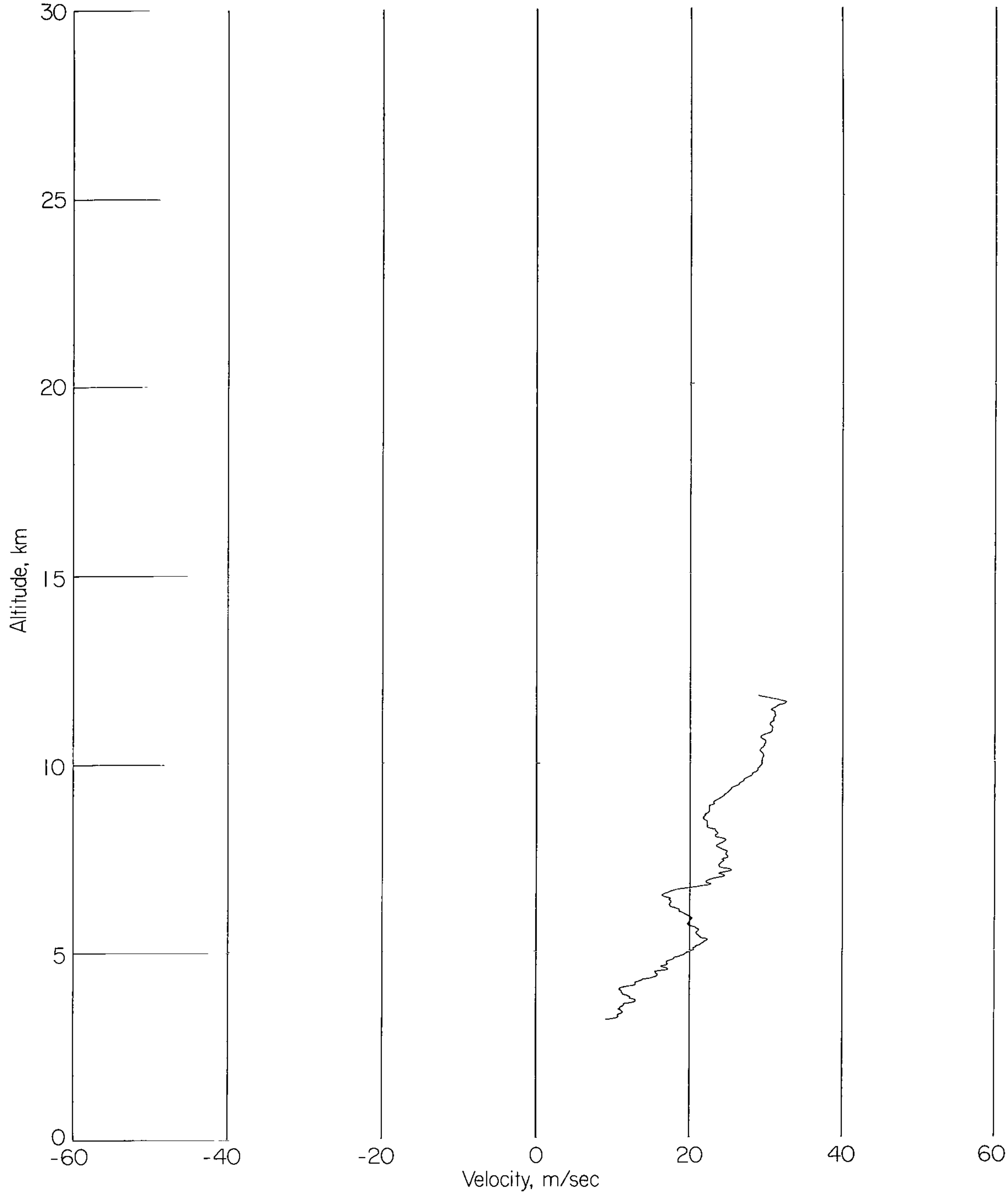

(a) West-to-east velocity component.

Figure 15.- Smoke-trail wind profile obtained on Nov. 22, 1961. Trail 019; time interval of 60 seconds; height interval of 25 meters.

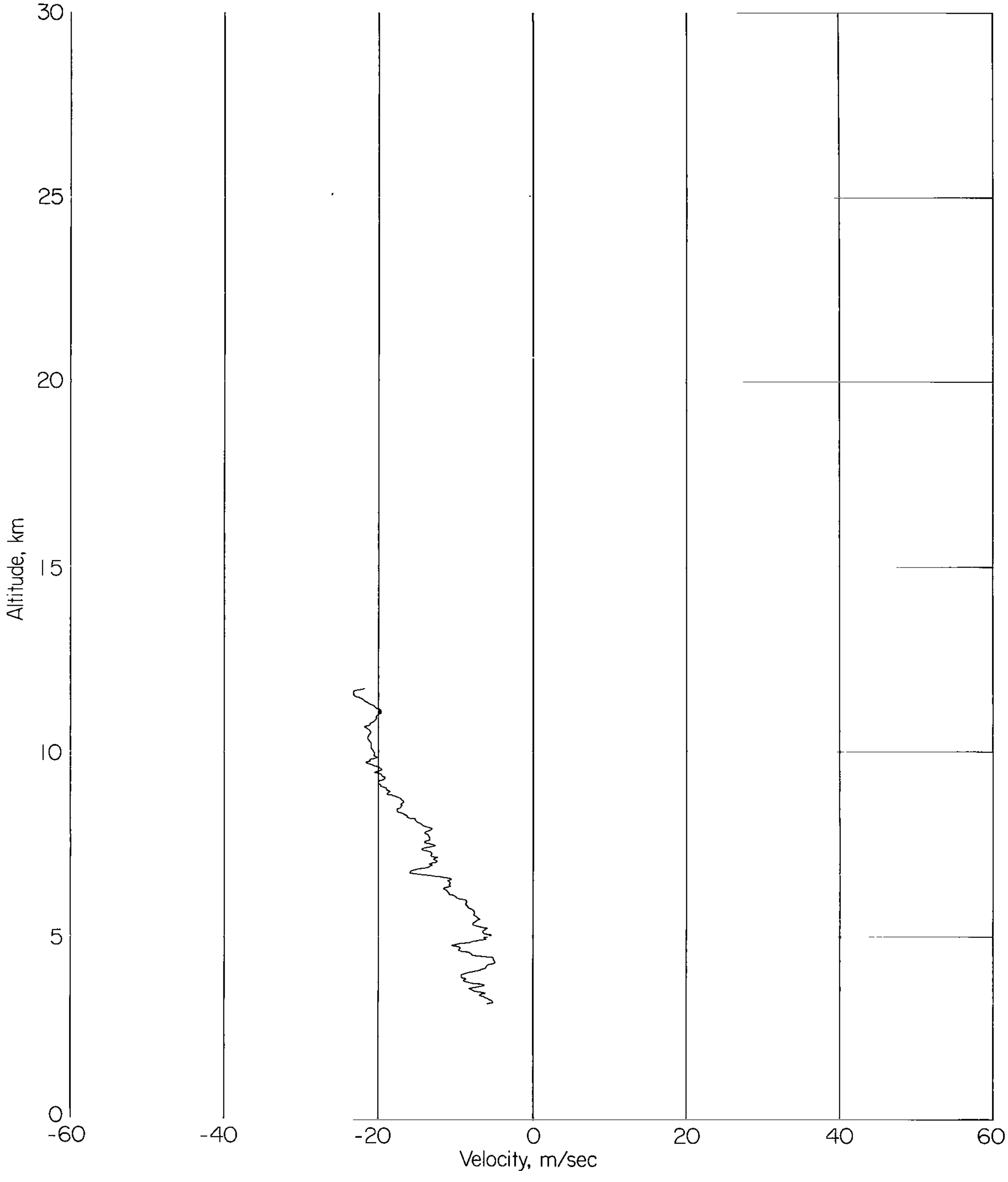

(b) South-to-north velocity component.

Figure 15.- Concluded.

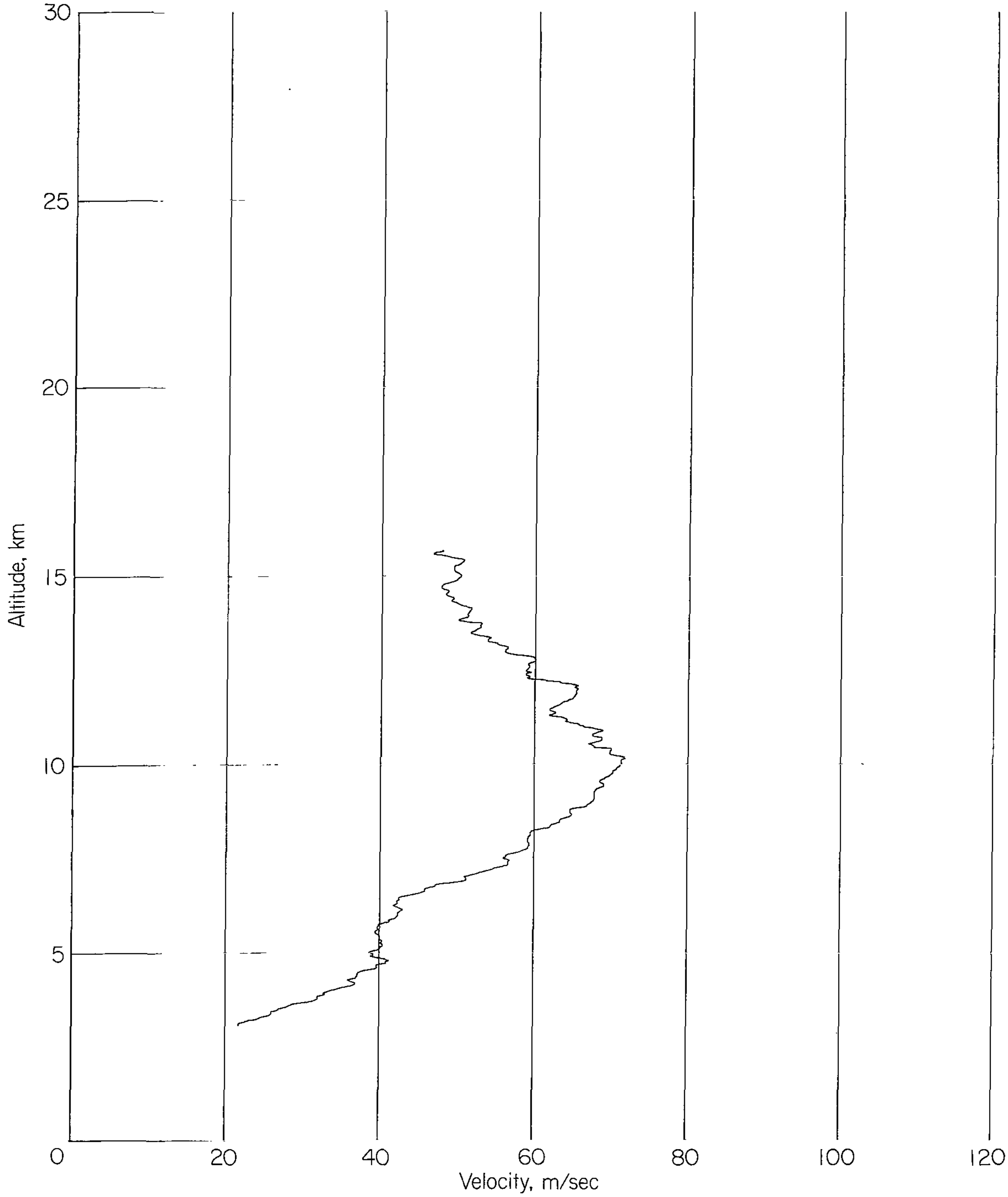

(a) West-to-east velocity component.

Figure 16.- Smoke-trail wind profile obtained on Jan. 16, 1962. Trail 020; time interval of 60 seconds; height interval of 25 meters.

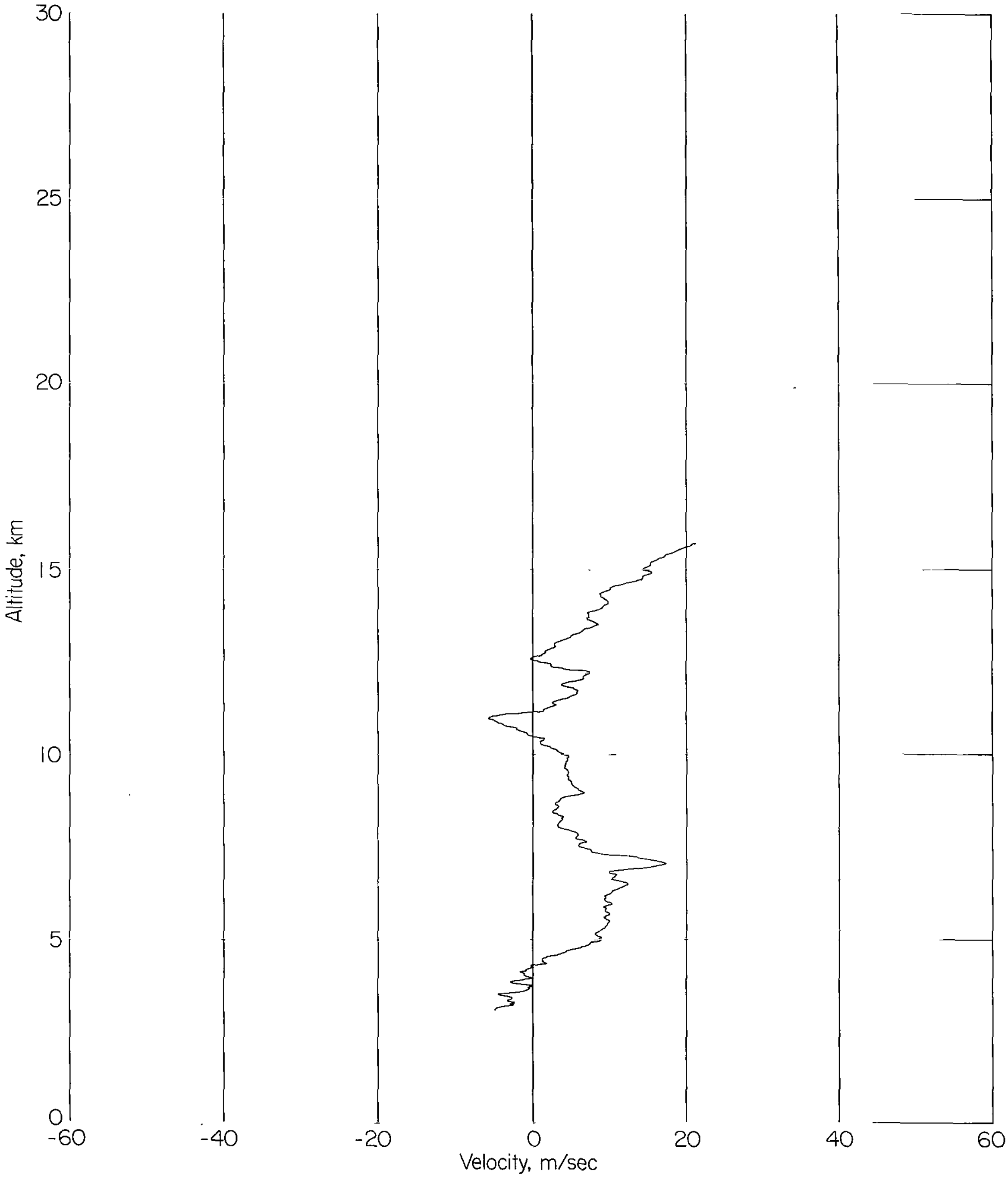

(b) South-to-north velocity component.

Figure 16.- Concluded.

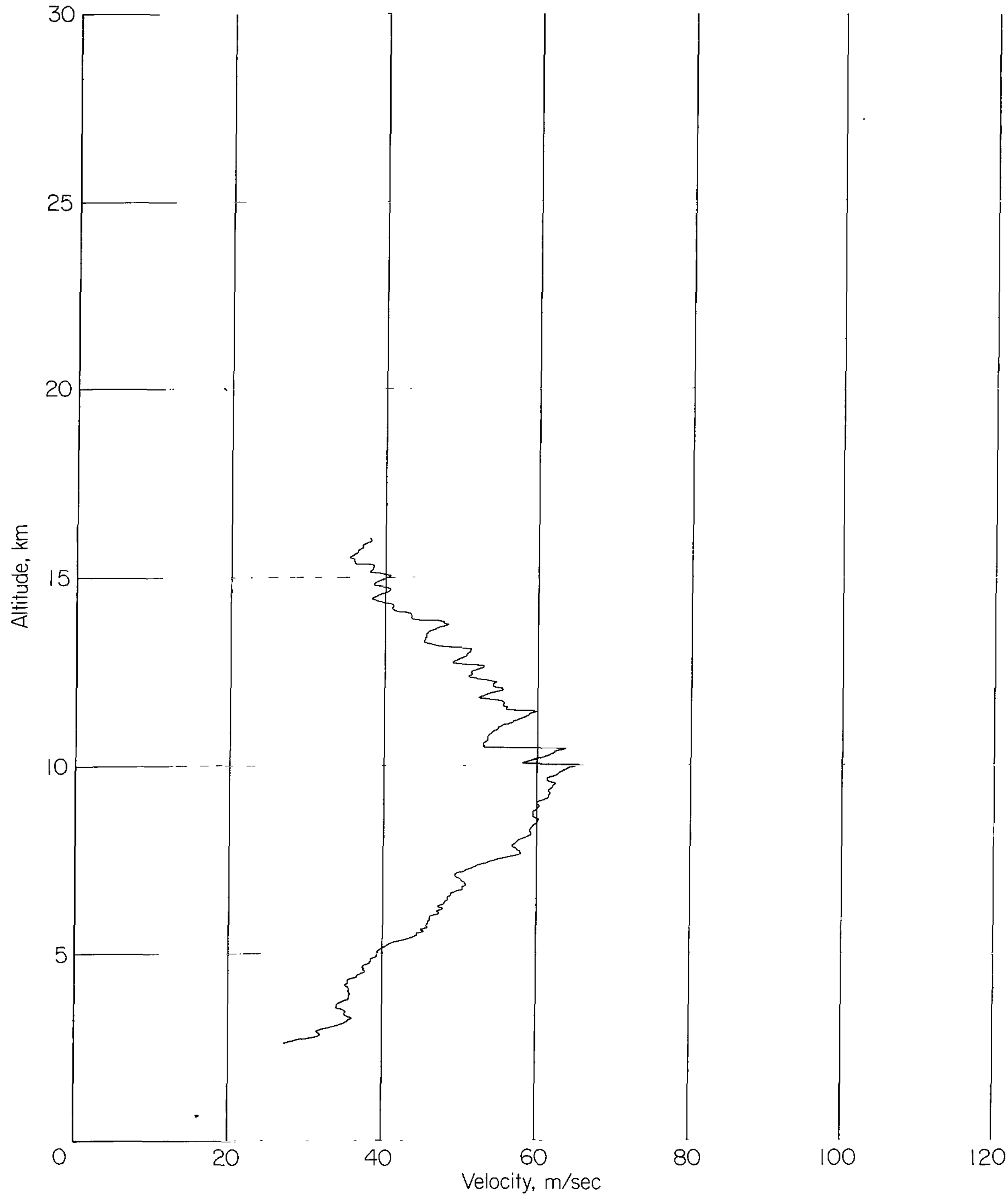

(a) West-to-east velocity component.

Figure 17.- Smoke-trail wind profile obtained on Feb. 6, 1962. Trail 021; time interval of 60 seconds; height interval of 25 meters.

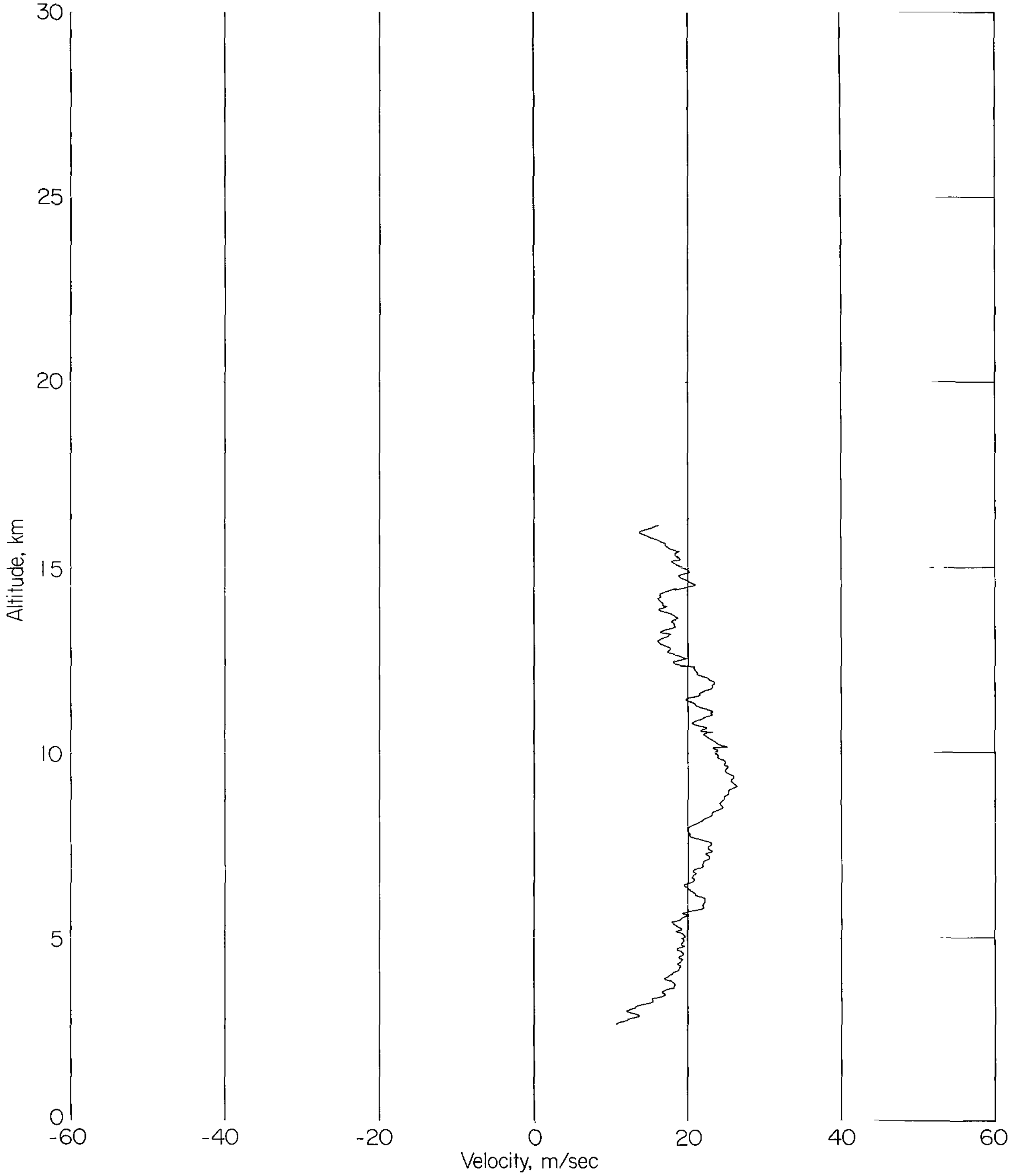

(b) South-to-north velocity component.

Figure 17.- Concluded.

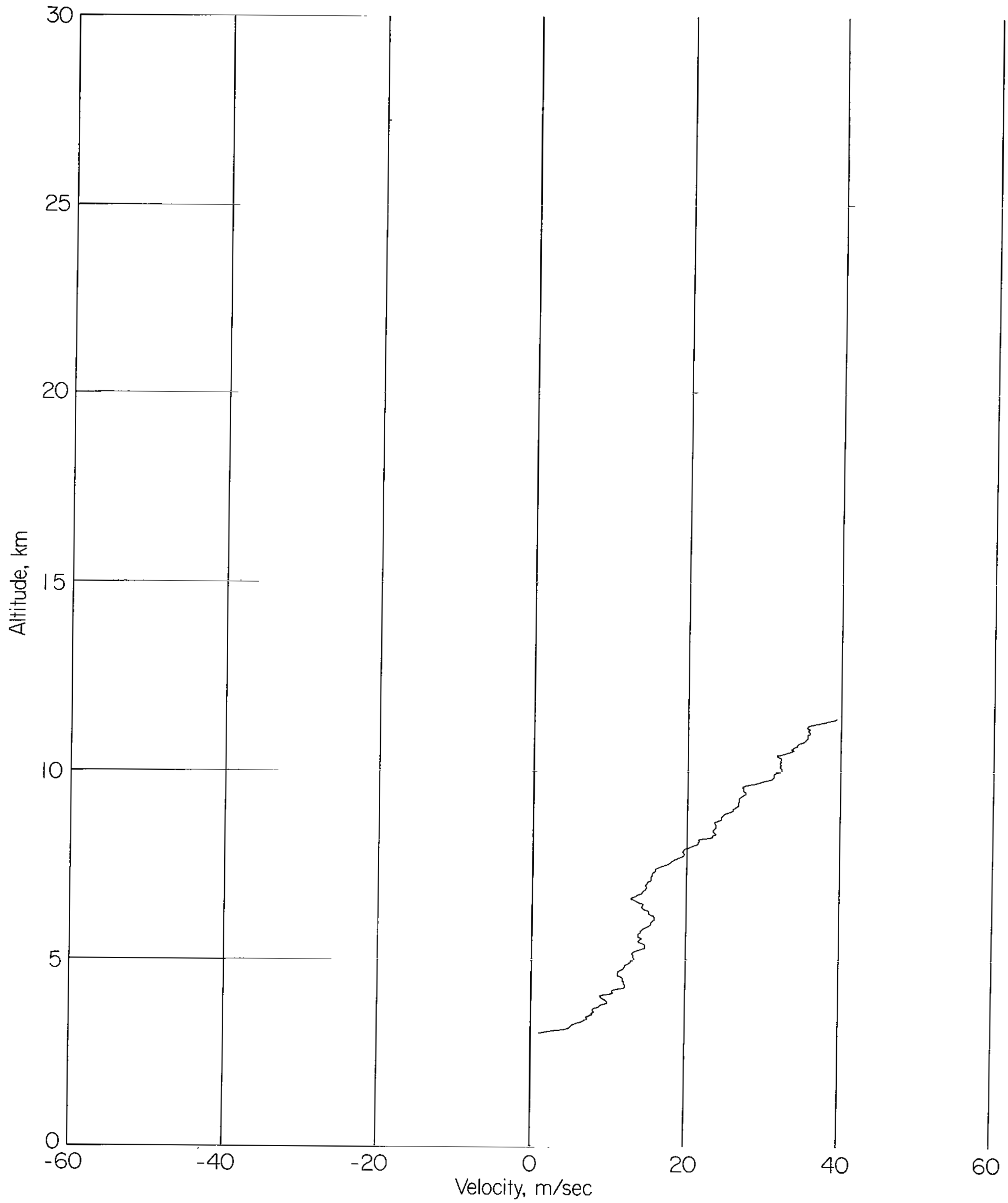

(a) West-to-east velocity component.

Figure 18.- Smoke-trail wind profile obtained on April 4, 1962. Trail 022; time interval of 60 seconds; height interval of 25 meters.

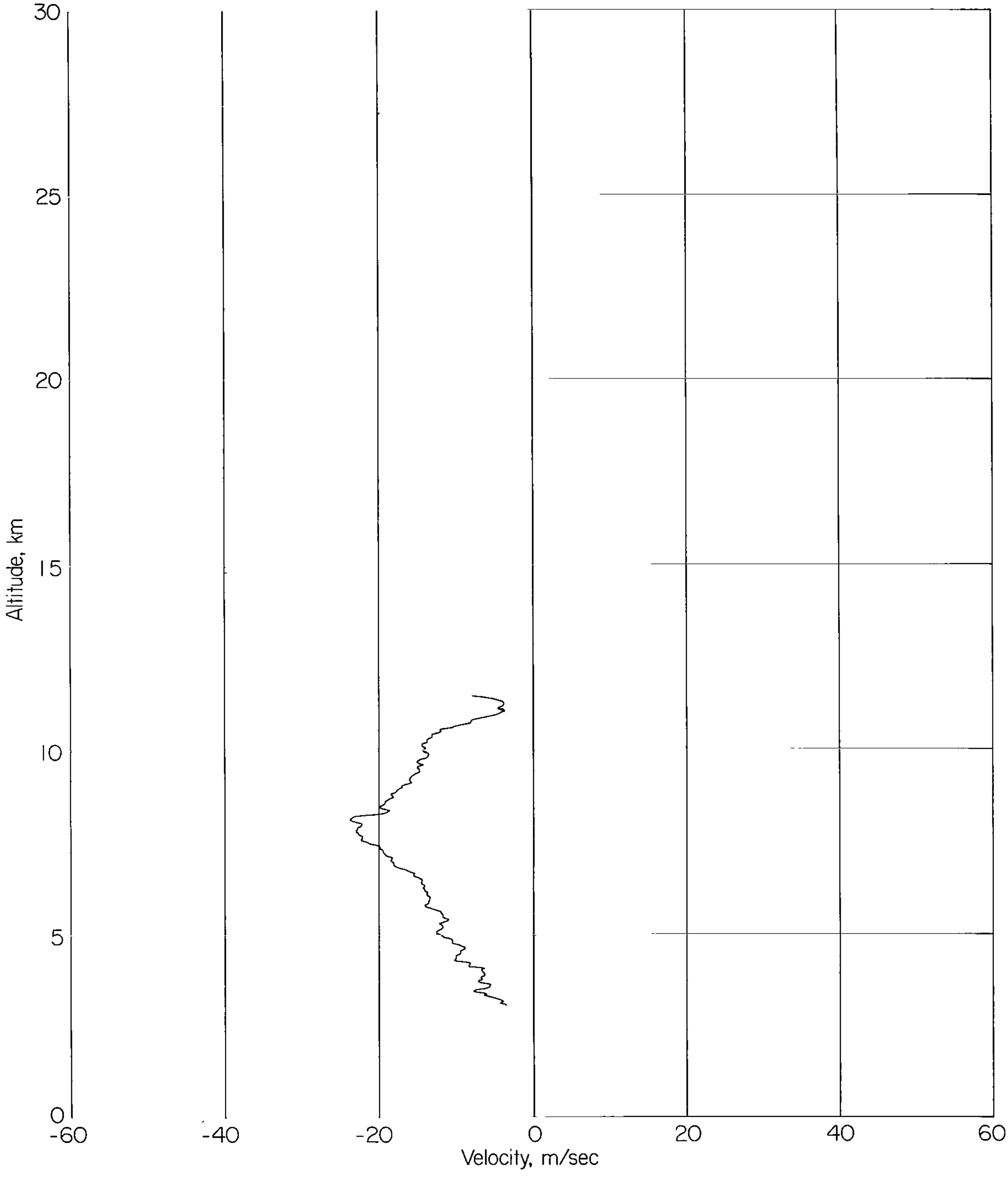

(b) South-to-north velocity component.

Figure 18.- Concluded.

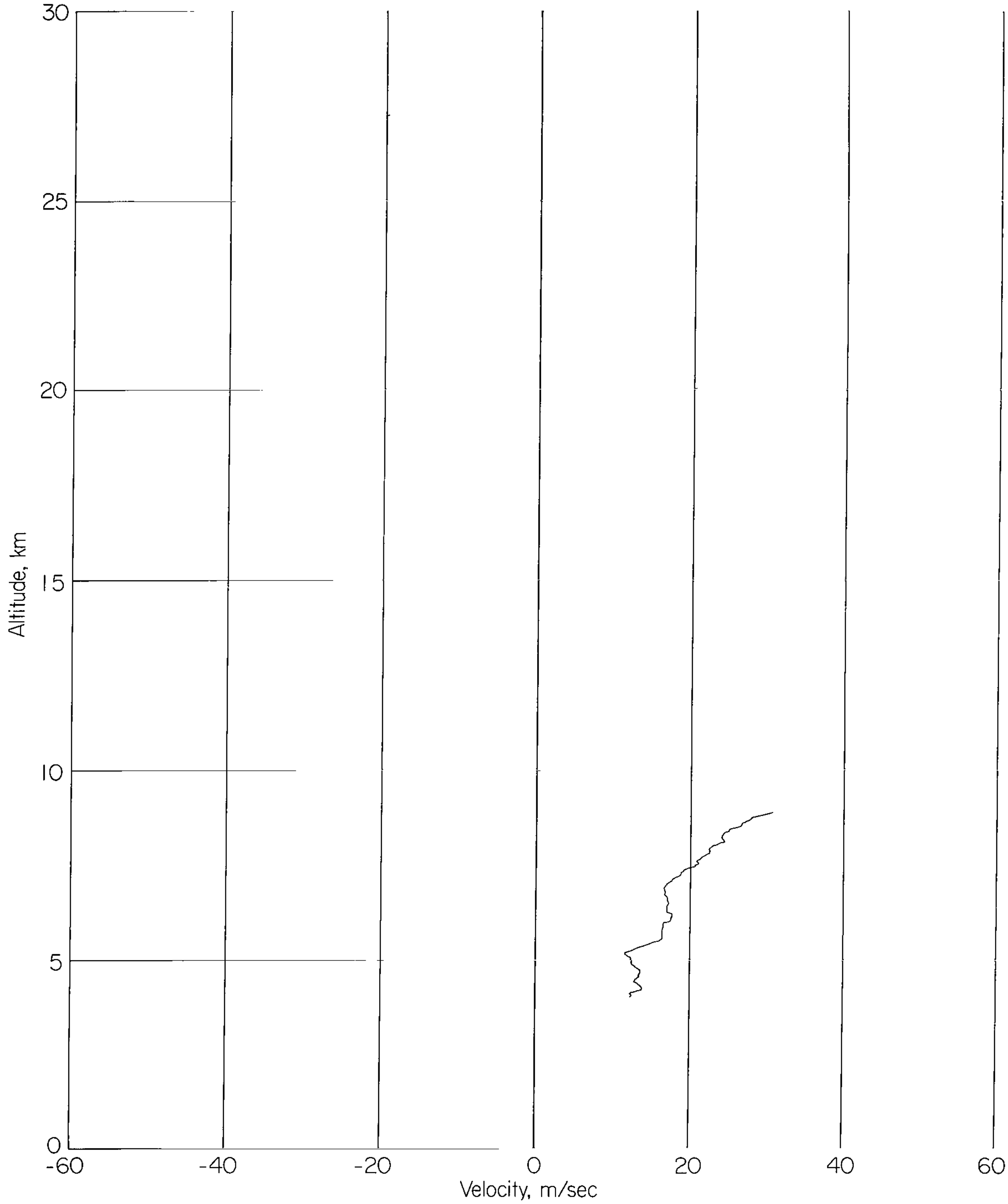

(a) West-to-east velocity component.

Figure 19.- Smoke-trail wind profile obtained on May 4, 1962. Trail 023; time interval of 60 seconds; height interval of 25 meters.

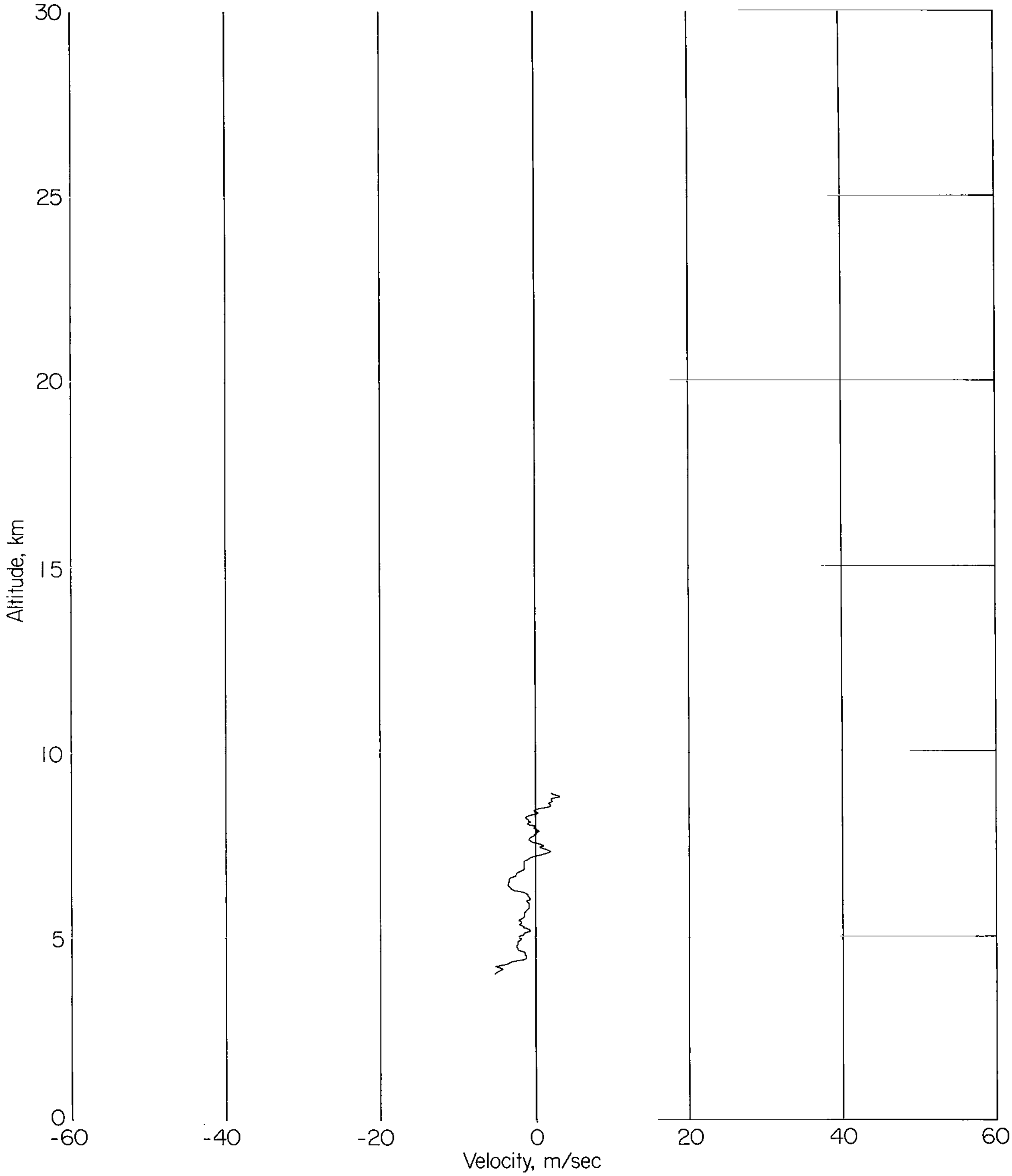

(b) South-to-north velocity component.

Figure 19.- Concluded.

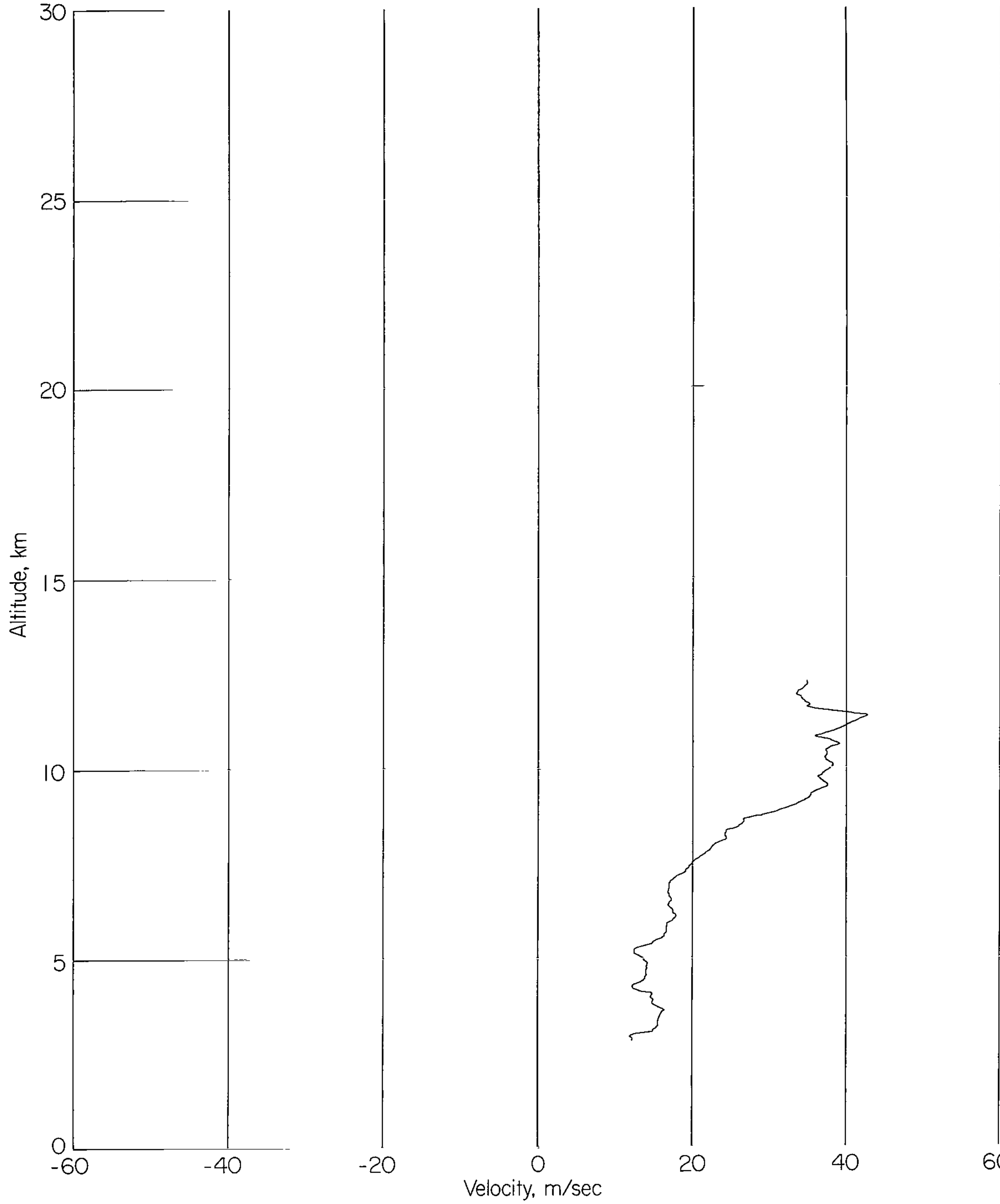

(a) West-to-east velocity component.

Figure 20.- Smoke-trail wind profile obtained on May 4, 1962. Trail 024; time interval of 60 seconds; height interval of 25 meters.

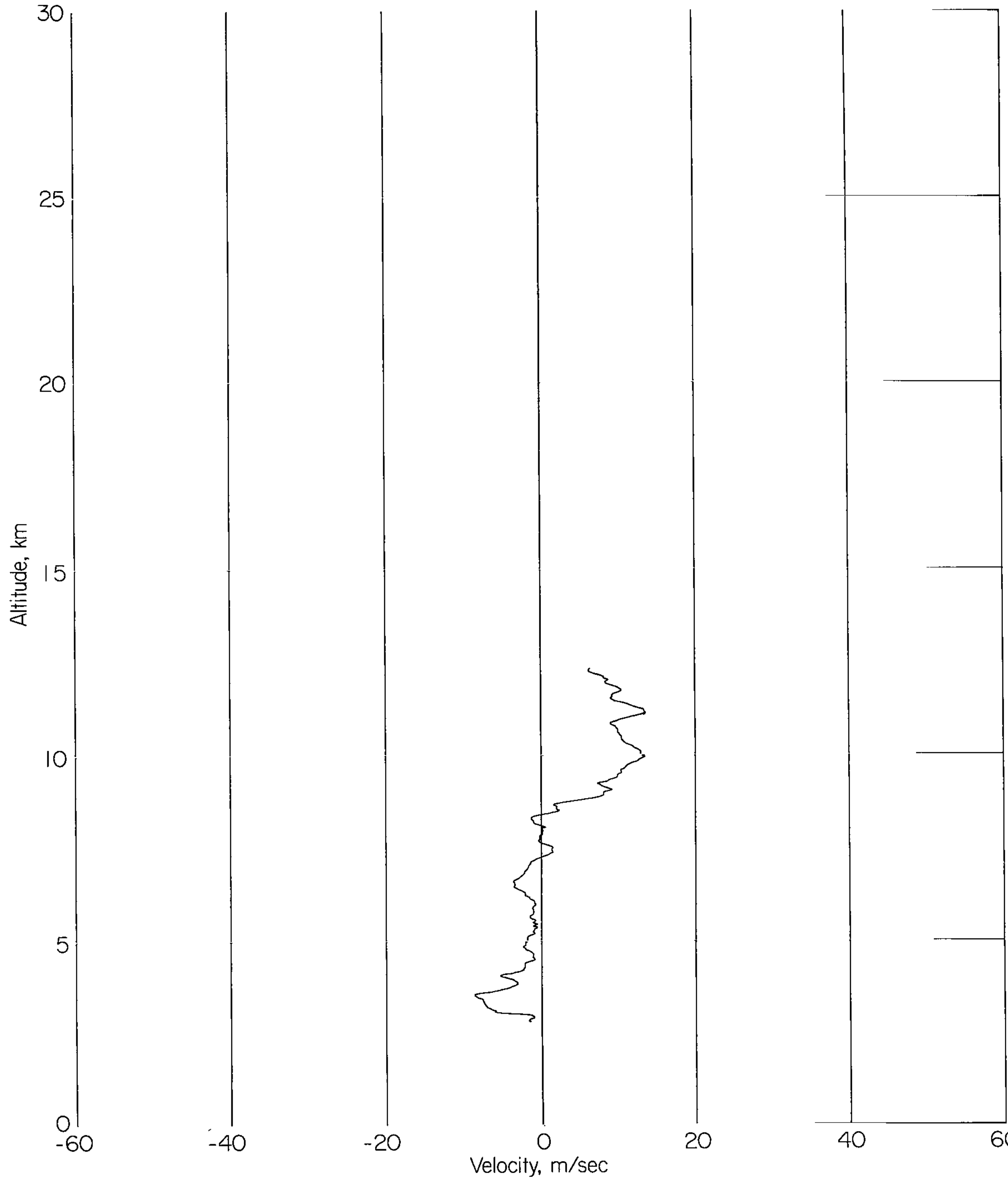

(b) South-to-north velocity component.

Figure 20.- Concluded.

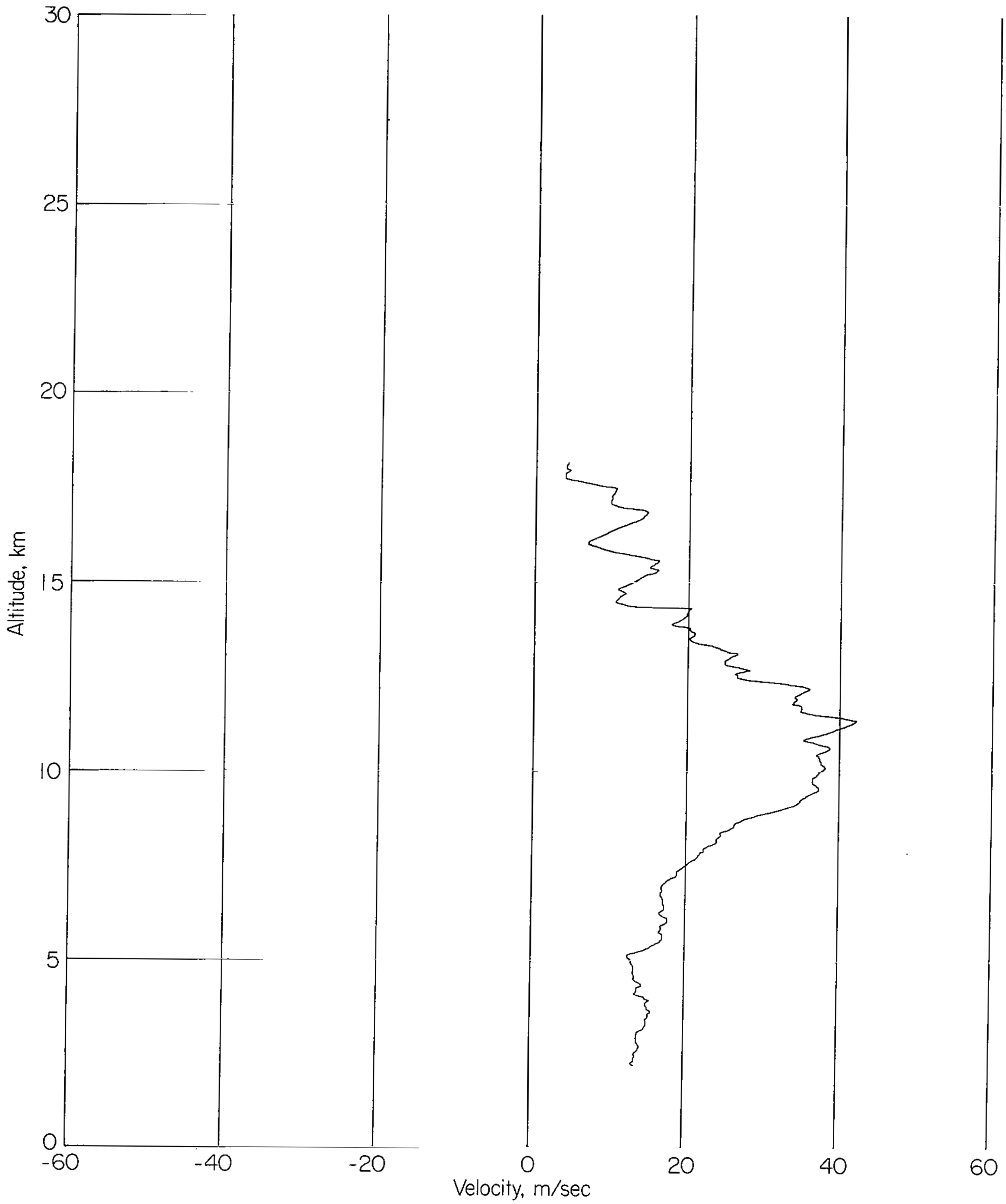

(a) West-to-east velocity component.

Figure 21.- Smoke-trail wind profile obtained on May 4, 1962. Trail 025; time interval of 60 seconds; height interval of 25 meters.

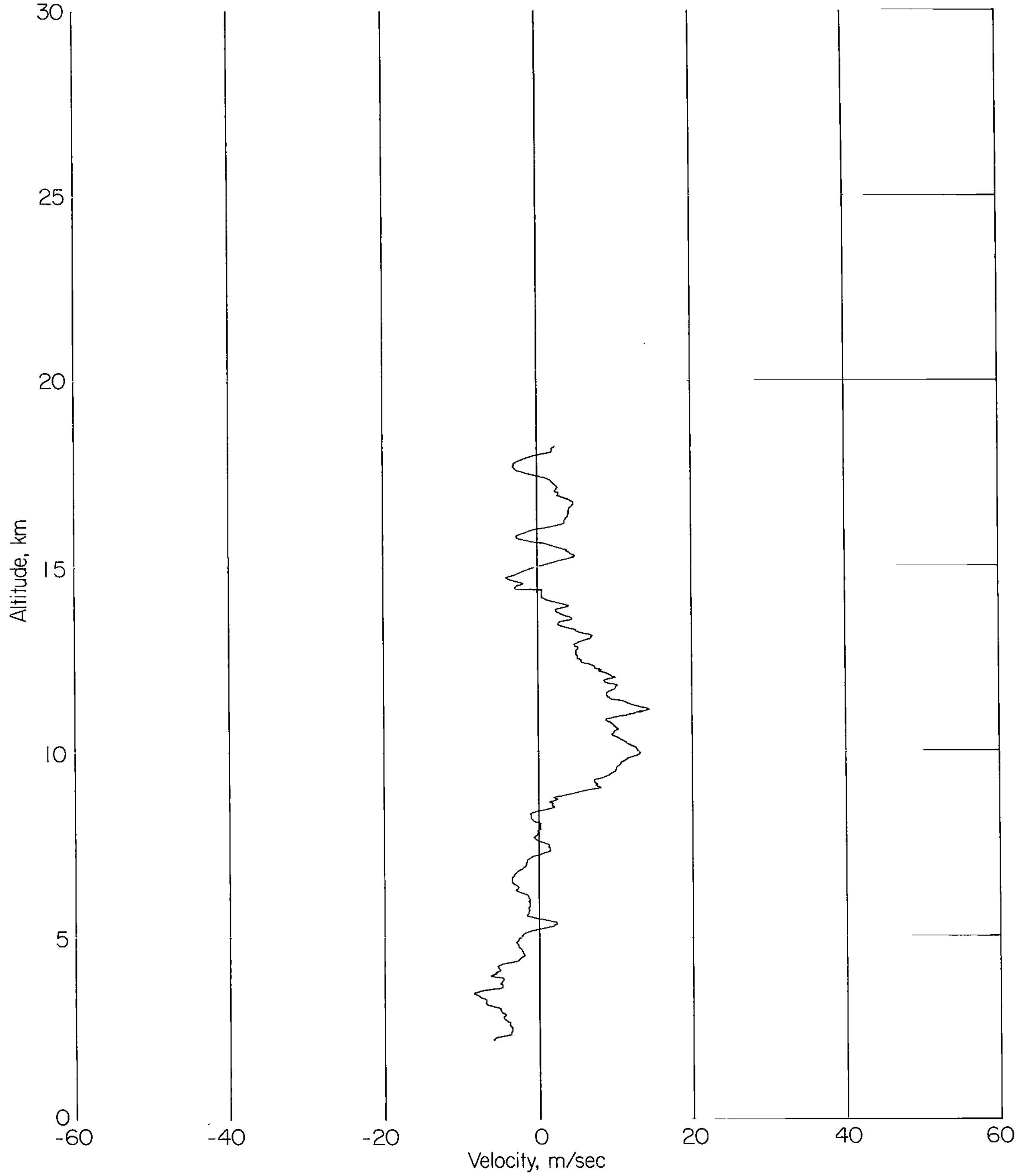

(b) South-to-north velocity component.

Figure 21.- Concluded.

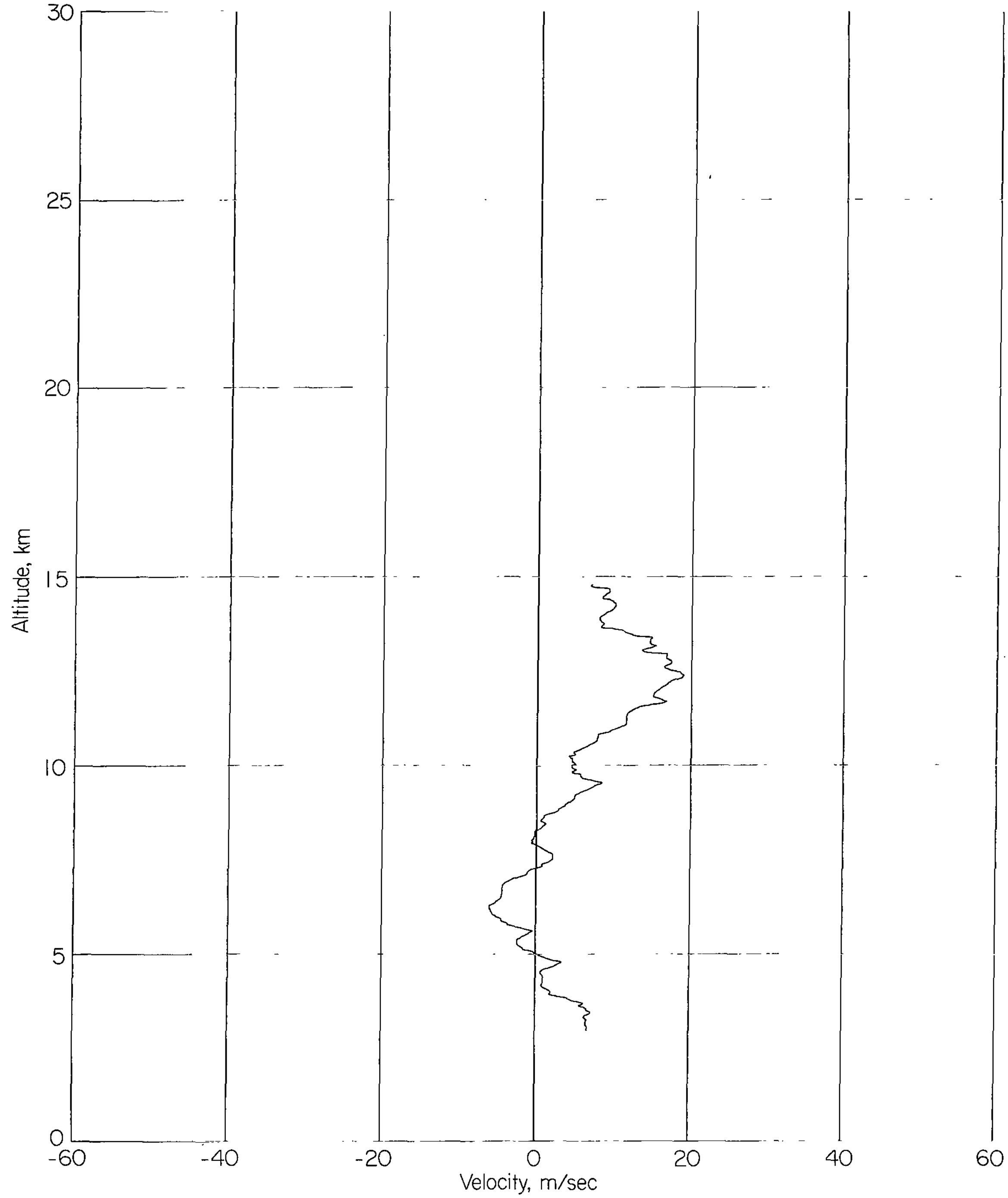

(a) West-to-east velocity component.

Figure 22.- Smoke-trail wind profile obtained on May 5, 1962. Trail 026; time interval of 60 seconds; height interval of 25 meters.

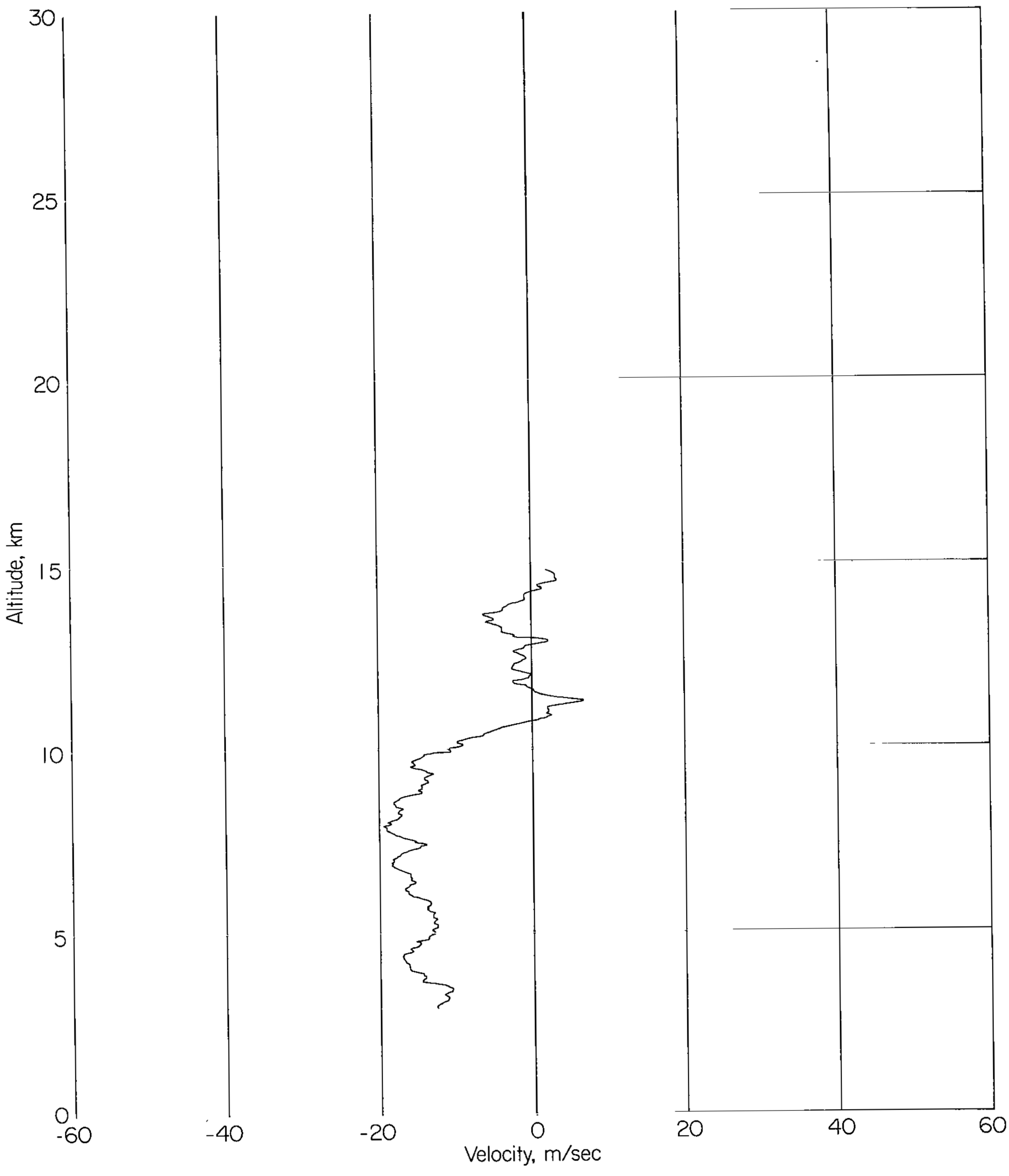

(b) South-to-north velocity component.

Figure 22.- Concluded.

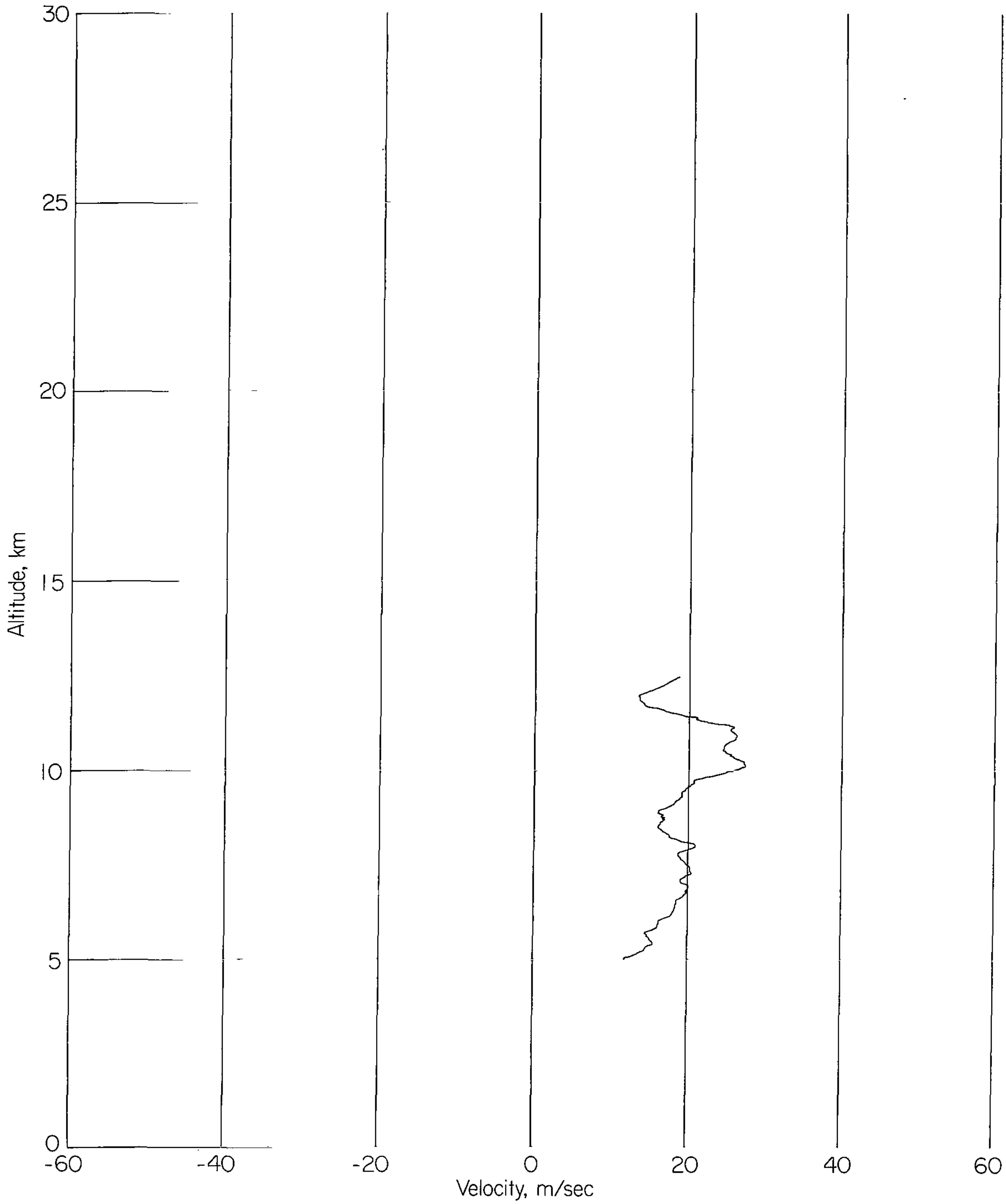

(a) West-to-east velocity component.

Figure 23.- Smoke-trail wind profile obtained on May 25, 1962. Trail 027; time interval of 60 seconds; height interval of 25 meters.

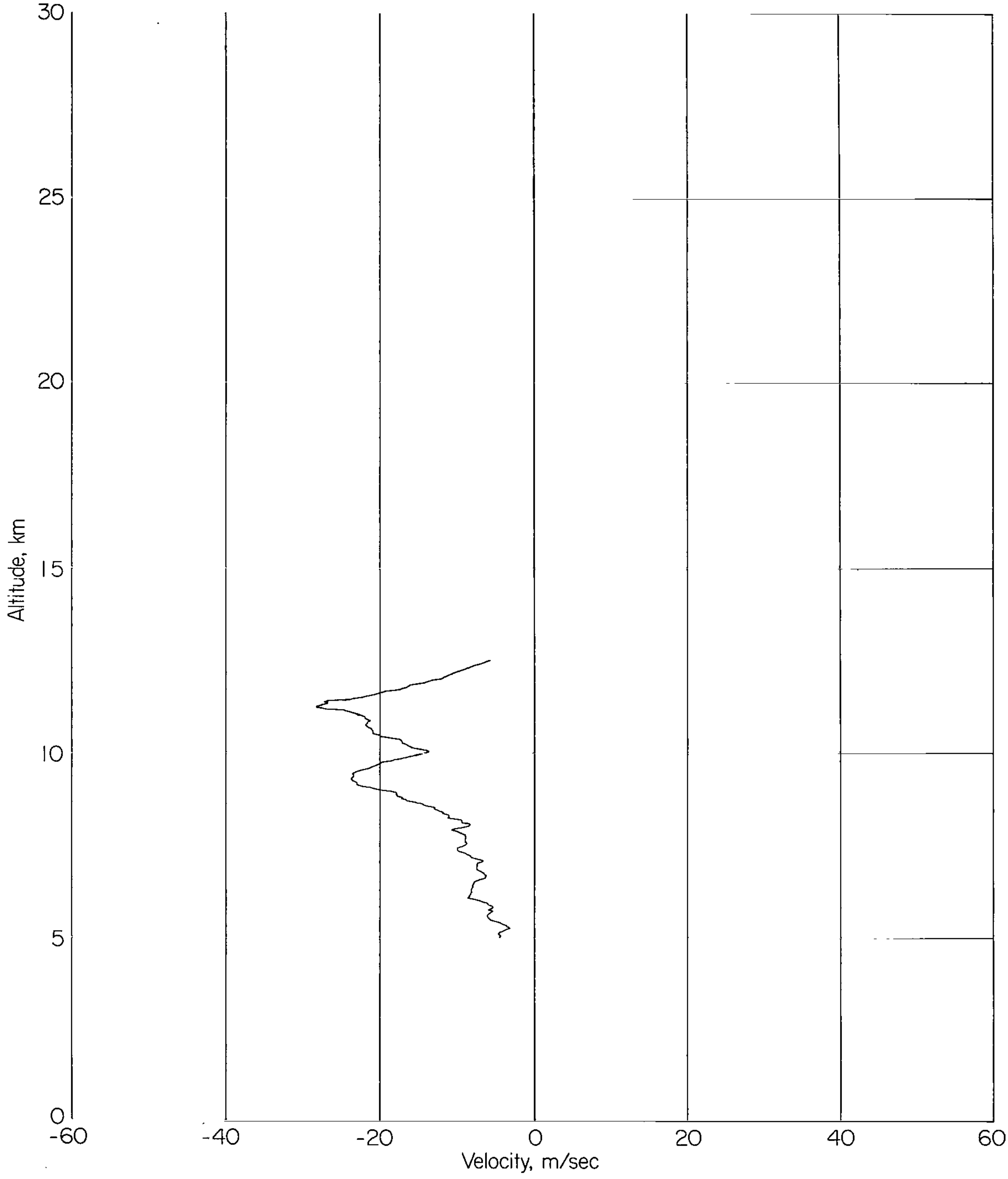

(b) South-to-north velocity component.

Figure 23.- Concluded.

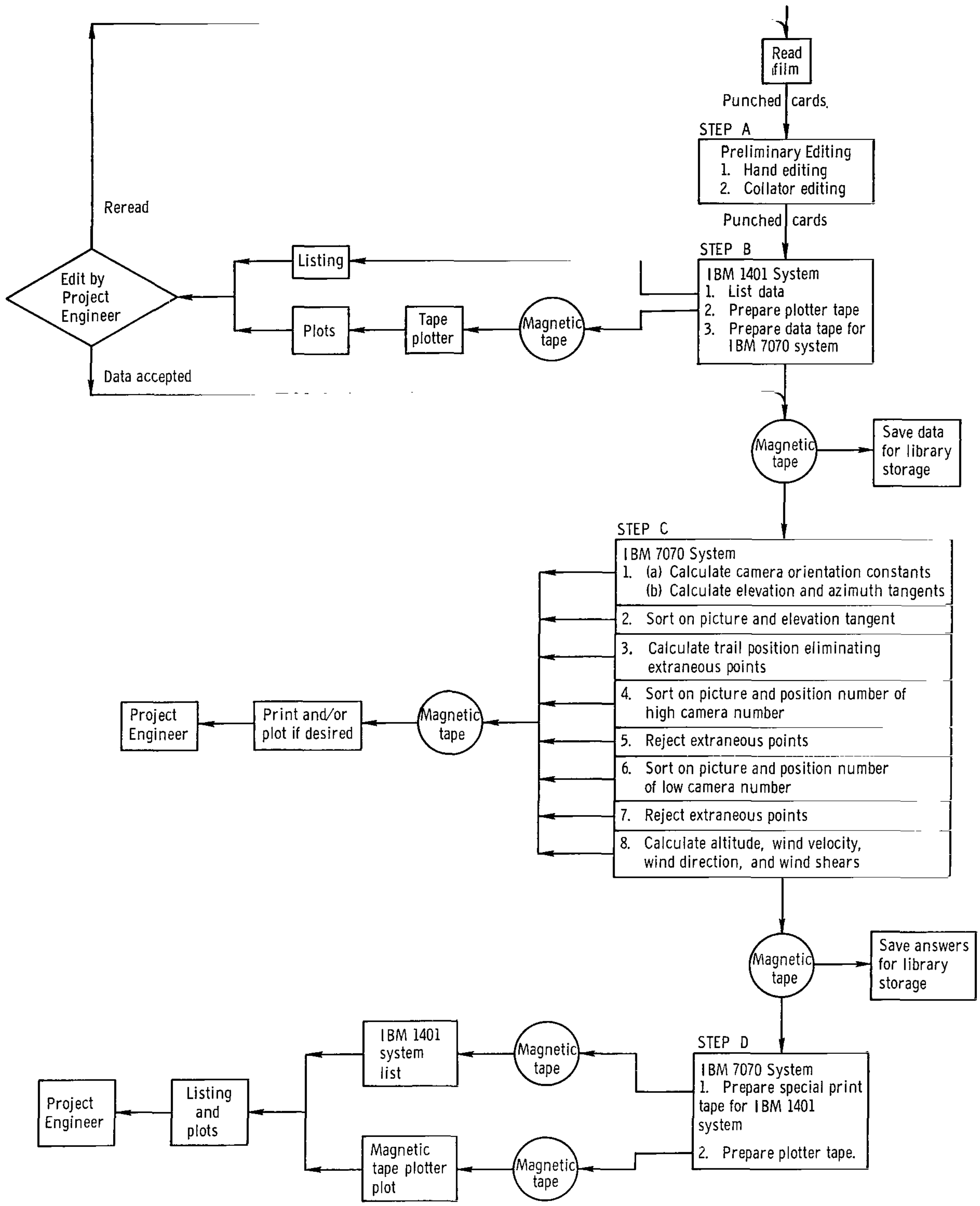

Figure 24.- Flow diagram of data reduction procedure.

NASA-Langley, 1965 L-4122